

J^+ -LIKE INVARIANTS OF PERIODIC ORBITS OF THE SECOND KIND IN THE RESTRICTED THREE BODY PROBLEM

JOONTAE KIM AND SEONGCHAN KIM

ABSTRACT. We determine three invariants: Arnold's J^+ -invariant as well as \mathcal{J}_1 and \mathcal{J}_2 invariants which were introduced by Cieliebak-Frauenfelder-van Koert, of periodic orbits of the second kind near the heavier primary in the restricted three body problem, provided that the mass ratio is sufficiently small.

CONTENTS

1. Introduction	1
2. Invariants of periodic orbits	3
3. The rotating Kepler problem	8
4. Computation of the J^+ -invariant	23
5. Computation of \mathcal{J}_1 and \mathcal{J}_2 invariants	27
References	30

1. INTRODUCTION

The planar circular restricted three body problem(PCR3BP) describes motions of a massless body under the influence of a Newtonian potential with two primaries. Because this system is not completely integrable, finding periodic orbits is not easy. One approach to attack this problem is finding families of periodic orbits. This approach was taken for example by Hill [12], Darwin [8, 9], Poincaré [16], Moulton [15], Ljapunov [13].

To find a starting point of a family of periodic orbits, one may vary dynamical systems. For example, if the mass ratio of the two primaries goes to either zero or one, the PCR3BP becomes in the limit the rotating Kepler problem which is completely integrable. Also, if one switches off the rotating term, then the PCR3BP becomes the Euler problem of two fixed centers which is also completely integrable. Since a periodic orbit in completely integrable systems is well known, one can take such a periodic orbit as a starting point of a family.

In this paper, we consider families of periodic orbits starting from the ones in the rotating Kepler problem by following the approach whose origin goes back to Poincaré. For such families, the parameter will be the mass ratio of the two primaries. Fixing the energy and varying the mass ratio, Poincaré obtained periodic orbits in the PCR3BP from periodic orbits in the rotating Kepler problem [16]. In the rotating Kepler problem, there are two kinds of periodic orbits: circular orbits and $T_{k,l}$ -type orbits(including collision orbits), where k, l are relatively prime. A circular orbit with a positive or a negative angular momentum is called the *retrograde circular orbit* or the *direct circular orbit*, respectively. They come from the retrograde and direct circular orbits in the inertial Kepler problem. On the other hand, $T_{k,l}$ -type orbits come from elliptic orbits in the inertial Kepler problem, more precisely they are k -fold Kepler ellipses in an l -fold rotating coordinate system. The family of $T_{k,l}$ -type orbits is called the *$T_{k,l}$ -torus family*. This family bifurcates from a $|k-l|$ -fold covered

Date: December 14, 2024.

direct circular orbit and ends at a $(k+l)$ -fold covered retrograde circular orbit, see Proposition 3.4. Note that the $T_{k,l}$ -torus family is in fact a 2-parameter family: one variable represents the rotational symmetry and the other one represents varying the eccentricity or equivalently the energy level of orbits. Since the rotation of periodic orbits does not affect the shape, without loss of generality we may think of the torus family as a 1-parameter family whose parameter is the eccentricity (or the energy level).

Poincaré defined two classes of periodic orbits in the PCR3BP obtained from the ones in the rotating Kepler problem: *periodic orbits of the first kind* which are obtained from the circular orbits and *periodic orbits of the second kind* which are obtained from $T_{k,l}$ -type orbits. The existence of periodic orbits of the first kind is discussed in detail by Birkhoff [6] and that of periodic orbits of the second kind by Arenstorf [3] and Barrar [5]. Note that in the $T_{k,l}$ -torus family, there exists a unique torus consisting of collision orbits. In [11], Giacaglia showed that even collision orbits can be continued to periodic orbits of the second kind. Moreover, if $k > 2\sqrt{2}l$, for a sufficiently small mass ratio the bifurcations of the $T_{k,l}$ -torus family from the circular orbits persist in the PCR3BP, more precisely the periodic orbits of the second kind bifurcate from a direct periodic orbit of the first kind and die at a retrograde periodic orbit of the first kind, see [17].

In order to apply holomorphic curve techniques in symplectic geometry to attack the dynamics, periodic orbits of the first kind are essential. Indeed, below the critical Jacobi energy direct and retrograde circular orbits bound (disk-like) global surfaces of section in the rotating Kepler problem [2] and in the PCR3BP for small mass ratios [14]. Moreover, the Conley-Zehnder indices of $T_{k,l}$ -type orbits can be computed from the Conley-Zehnder indices of the circular orbits, see [2].

In this paper, however, we are interested in periodic orbits of the second kind and determine their invariants. Since they are planar curves, a natural candidate for an invariant is Arnold's J^+ -invariant [4]: an invariant of families of planar immersions which does not change under crossings through triple intersections and inverse self-tangencies. Hence, it provides an invariant for families of periodic orbits with finitely many triple intersections and inverse self-tangencies. Note that this invariant behaves sensitive under direct self-tangencies, see Section 2.2.

However, in a family of periodic orbits in the PCR3BP the particle can collide with one of the primaries or touch the boundary of the Hill's region. For the former disaster, denoted by (I_0) , birth or death of loops around the primary happens. For the latter one, birth or death of interior or exterior loops (depending on the connected component of the Hill's region in which the periodic orbit lies) happens. To see this picture more precisely, recall that if the energy is less than the first critical value, the Hill's region consists of three connected components: two bounded components and one unbounded component. If the latter disaster happens in one of the bounded components, then birth or death of exterior loops through cusps at the boundary of the Hill's region occurs, which we denote by (I_∞) . If the disaster happens in the unbounded component, then we see a similar picture with interior loops instead of exterior loops, which we denote by $(I_{-\infty})$. This phenomenon occurs in more general systems, i.e., Stark-Zeeman systems, see Section 2.4. Note that Arnold's J^+ -invariant does not change under (I_∞) , but it does change under (I_0) and $(I_{-\infty})$. This implies that the J^+ -invariant is not a suitable invariant for families of periodic orbits in the PCR3BP.

Recently, Cieliebak-Frauenfelder-van Koert introduced two invariants [7]: \mathcal{J}_1 and \mathcal{J}_2 invariants, for families of periodic orbits in Stark-Zeeman systems which are also invariant under (I_0) . These two invariants are based on Arnold's J^+ -invariant, more precisely the \mathcal{J}_1 invariant is defined by a combination of the J^+ -invariant and the winding number of a periodic orbit which plays a role in correcting errors arising from birth or death of additional loops. On the other hand, the \mathcal{J}_2 invariant is defined as the J^+ -invariant of the pulled back image of a periodic orbit under the Levi-Civita embedding. Note that all three invariants J^+ , \mathcal{J}_1 and \mathcal{J}_2 do not depend on the choice of the orientation of an orbit.

The main result of this paper is to determine the invariants of families of periodic orbits of the second kind in the PCR3BP:

Theorem 1.1. *Let α be a $T_{k,l}$ -type orbit with $k > l$. Then there exists a small $\mu_{k,l} > 0$ such that for each $\mu < \mu_{k,l}$ all periodic orbits δ of the second kind near the heavier primary in the restricted three body problem, which are obtained from α , satisfy:*

$$\begin{aligned}\mathcal{J}_1(\delta) &= 1 - k + \frac{k^2}{2} - \frac{l^2}{2} \\ \mathcal{J}_2(\delta) &= \begin{cases} (k-1)^2 - l^2 & \text{if the winding number of } \delta \text{ is odd,} \\ 1 - k + \frac{k^2}{4} - \frac{l^2}{4} & \text{if the winding number of } \delta \text{ is even.} \end{cases}\end{aligned}$$

In particular, the 1-parameter $T_{k,l}$ -torus family is of Stark-Zeeman type and hence all periodic orbits obtained from $T_{k,l}$ -type orbits have the same \mathcal{J}_1 and \mathcal{J}_2 invariants.

Remark 1.2. In Sections 4 and 5 we also provide formulas for the two invariants \mathcal{J}_1 and \mathcal{J}_2 for $k < l$ and the J^+ -invariant for any k and l .

Remark 1.3. The formulas in Theorem 1.1 fit well to the relation $\mathcal{J}_2(\delta) = 2\mathcal{J}_1(\delta) - 1$, provided that the winding number δ is odd, which is given in [7, Proposition 6]). Indeed, we compute that

$$\begin{aligned}\mathcal{J}_2(\delta) &= 2\mathcal{J}_1(\delta) - 1 \\ &= 2\left(1 - k + \frac{k^2}{2} - \frac{l^2}{2}\right) - 1 \\ &= 1 - 2k + k^2 - l^2 \\ &= (k-1)^2 - l^2.\end{aligned}$$

Acknowledgements: We would like to express our deepest gratitude to Urs Frauenfelder for fruitful discussions. This work was carried out while J. Kim was visiting University of Augsburg and he is grateful to his supervisor Otto van Koert for continued support and encouragement. We also would like to thank the Institute for Mathematics of University of Augsburg for providing a supportive research environment. J. Kim is supported by the NRF Grant NRF-2016R1C1B2007662 funded by the Korean government and S. Kim by DFG grants CI 45/8-1 and FR 2637/2-1.

2. INVARIANTS OF PERIODIC ORBITS

In this section, we briefly recall some relevant parts of the three invariants J^+ , \mathcal{J}_1 and \mathcal{J}_2 of plane curves. We also introduce the Viro's formula for the J^+ -invariant, which is useful for the computational purpose.

2.1. Immersions in the plane. Since we are interested in (simple covered) planar periodic orbits, throughout the paper a curve always means a map $\gamma : S^1 \rightarrow \mathbb{C}$ from the circle into the complex plane. By an *immersion*, we mean an immersed curve $\gamma : S^1 \rightarrow \mathbb{C}$ which is considered up to orientation preserving reparametrization. By abusing the notation, an immersion is identified with its image $K := \gamma(S^1) \subset \mathbb{C}$. Along an immersion, there might exist a double point at which the tangent vectors are parallel. This event is called a *direct self-tangency* (or an *inverse self-tangency*) if the two tangent vectors point in the same direction (or in the opposite directions). An immersion is said to be *generic* if it has no triple points and no self-tangencies, so it has only transverse double points. By a *generic homotopy* $(K^s)_{s \in [0,1]}$, we mean a homotopy of immersions with finitely many $s \in (0,1)$ at which three disasters in Figure 1 can occur. Note that in particular under the crossing through a self-tangency the number of double points changes.

2.2. Arnold's J^+ -invariant. Arnold's J^+ -invariant, denoted by $J^+(K) \in 2\mathbb{Z}$ for a generic immersion $K \subset \mathbb{C}$, is an invariant that is characterized by the following properties:

- (i) it is independent of the orientation;
- (ii) it does not change under the crossing through an inverse self-tangency or a triple point;

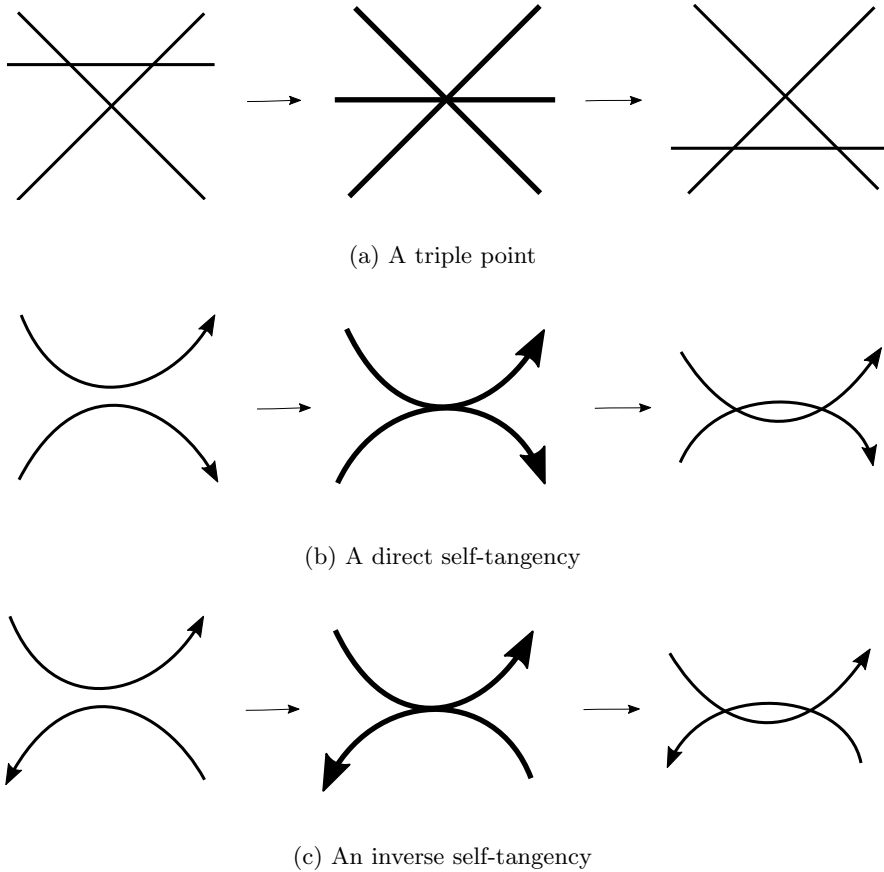


FIGURE 1. Three disasters which can occur during a generic homotopy

- (iii) it increases by two under the crossing through a positive (increasing the number of double points) direct self-tangency, see Figure 1b;
- (iv) define standard curves K_j , $j \in \mathbb{Z}_{\geq 0}$, as follows: K_0 is the figure eight and for each $j \neq 0$, the curve K_j is the circle with $(j-1)$ interior loops whose rotation number equals j , where the rotation number of a curve is defined to be the winding number of the tangent vector. In Figure 2 we illustrate some examples of the standard curves. We then have

$$J^+(K_j) = \begin{cases} 2-2j & j \neq 0, \\ 0 & j = 0. \end{cases}$$

Note that the J^+ -invariant exists and is uniquely defined by the above properties. Moreover, it is additive under connected sums, see [4, Chapter 1].

2.3. Viro's formula. For a generic immersion $K \subset \mathbb{C}$, we let Λ_K be the *set of all connected components of the complement* $\mathbb{C} \setminus K$ and let D_K be the *set of all double points of* K . The *winding number of* K *around a component* $C \in \Lambda_K$, denoted by $w_C(K)$, is defined to be the winding number of K around an interior point in C . Note that this number does not depend on the choice of the interior point, so $w_C(K)$ is well-defined. In order to define the index of a double point, we observe that every double point is adjacent to four components (possibly with a multiple component). The *index of* K *at the double point* $p \in D_K$, denoted by $\text{ind}_p(K)$, is then defined to be the arithmetic mean of the winding numbers of the adjacent to four components. We now state the Viro's formula.

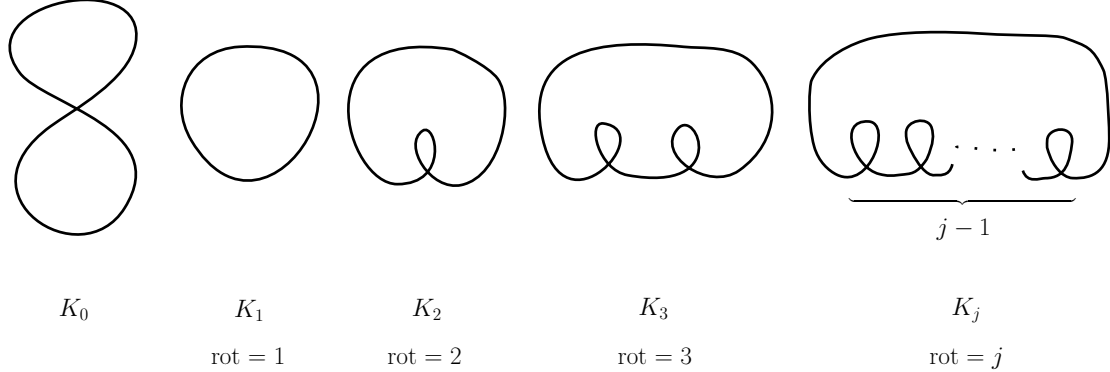


FIGURE 2. The standard curves

Theorem 2.1. Let K be a generic immersion with n double points. Then Arnold's J^+ -invariant of K is given by

$$J^+(K) = 1 + n - \sum_{C \in \Lambda_K} (w_C(K))^2 + \sum_{p \in D_K} (ind_p(K))^2.$$

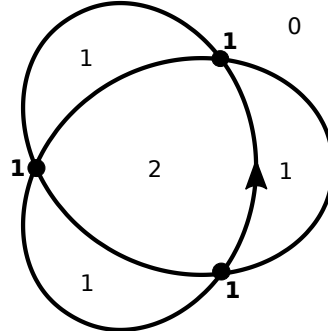
This was proven in [18, Corollary 3.1.B and Lemma 3.2.A]. This formula tells us that the information of all double points and the winding number around each component of the complement completely determines the J^+ -invariant.

Example 2.2. We compute the J^+ -invariant of a generic immersion $K \subset \mathbb{C}$ given in Figure 3. We assume that K has the counter-clockwise orientation. The complement $\mathbb{C} \setminus K$ has 5 components (including the unbounded component) and the number in the interior of each component means its winding number. The immersion has three double points, and the index at each double point is given by

$$\frac{1}{4} \cdot (0 + 1 + 1 + 2) = 1.$$

By the Viro's formula, we obtain

$$J^+(K) = 1 + 3 - (3 \cdot 1^2 + 1 \cdot 2^2 + 1 \cdot 0^2) + (3 \cdot 1^2) = 0.$$


 FIGURE 3. A generic immersion $K \subset \mathbb{C}$

Example 2.3. In Figure 4, there is a double point which is adjacent to four component with a multiple component of winding number 1. The index of the double point is given by

$$\frac{1}{4} \cdot (0 + 1 + 1 + 2) = 1.$$

Hence, we obtain

$$J^+(K) = 1 + 1 - (1^2 + 2^2) + 1^2 = -2.$$

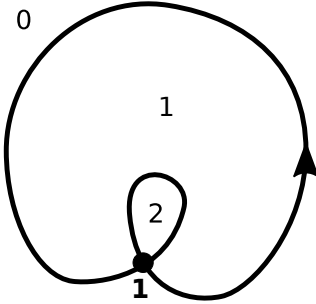


FIGURE 4. A generic immersion $K \subset \mathbb{C}$

It is worth mentioning that the winding number around the unbounded component is always zero for any generic immersion.

2.4. The \mathcal{J}_1 and \mathcal{J}_2 invariants. In the paper [7], Cieliebak, Frauenfelder and van Koert defined the two J^+ -like invariants \mathcal{J}_1 and \mathcal{J}_2 of 1-parameter families of simple periodic orbits in (planar) Stark-Zeeman systems. A *Stark-Zeeman system* is a Hamiltonian system whose Hamiltonian is given by the Hamiltonian of the Kepler problem added by some potential and magnetic terms, where a potential term depends only on the position and a magnetic term also depends on the momentum. For example, the restricted three-body problem and the rotating Kepler problem, which we treat in this paper, are Stark-Zeeman systems, see [7, Section 3.2]. In what follows, we assume that the magnetic term is nonzero and nonsingular.

Fix the energy level $c < c_1$, where $c_1 \in \mathbb{R} \cup \{\infty\}$ is the first critical value of the Hamiltonian of a Stark-Zeeman system. Recall that the *Hill's region* \mathcal{K}_c is defined to be the projection of the energy hypersurface to the configuration space. Physically, the Hill's region is a region in the configuration space in which the massless body of the associated energy can lie. In particular, velocity of the particle vanishes if and only if the particle lies on the boundary of the Hill's region. Since we have fixed $c < c_1$, it contains a unique bounded component \mathcal{K}_c^b which is diffeomorphic to a closed disk except for the origin. We now regularize the system so that periodic orbits are allowed to pass through the origin. Note that the regularized bounded component of the Hill's region, which we again denote by \mathcal{K}_c^b , is diffeomorphic to a closed disk. We denote by \mathcal{K}_c^u the unbounded component of the Hill's region.

Consider an orbit $q : \mathbb{R} \rightarrow \mathbb{R}^2$ in \mathcal{K}_c^b and fix a point $q_0 = q(t_0)$. Then it satisfies one of the following:

- (i) $q_0 \in \text{int}(\mathcal{K}_c^b) \setminus \{(0, 0)\}$: in this case, the velocity $\dot{q}(t_0)$ does not vanish and hence the orbit q is an immersion near q_0 ;
- (ii) $q_0 \in \partial\mathcal{K}_c = \partial\mathcal{K}_c^b \cup \partial\mathcal{K}_c^u$: recall that on the boundary of the Hill's region, the velocity vanishes. Cieliebak-Frauenfelder-van Koert showed that in this situation the orbit q has a cusp at $t = t_0$, see [7, Lemma 1]. Moreover, if q is a member of a 1-parameter family q^s of nearby orbits of the same energy with $q^0 = q$, then through the cusp birth or death of an exterior loop can occur, see Figures 5b, 5e;

(iii) $q_0 = (0, 0)$: similar to the previous case, the orbit has a cusp at $t = t_0$. If the orbit is a member of the 1-parameter family described as in the previous case, then through the cusp birth or death of a loop around the origin can occur, see [7, Lemma 2] and Figure 5a.

Because of the additivity under connected sum, the event (ii) for $\partial\mathcal{K}_c^b$ above does not influence on the J^+ -invariant. However, through the event (ii) for $\partial\mathcal{K}_c^u$ or (iii), the J^+ -invariant can change. This implies that a 1-parameter family of periodic orbits in a Stark-Zeeman system is not just a generic homotopy and the J^+ -invariant is not a suitable invariant for this family. In view of the discussions so far, Cieliebak-Frauenfelder-van Koert introduced the following notion which is a generalization of a generic homotopy.

Definition 2.4. ([7, Definition 1]) A 1-parameter family $(K^s)_{s \in [0,1]}$ of closed curves in \mathbb{C} is called a **Stark-Zeeman homotopy** if each K^s is a generic immersion in $\mathbb{C}^* = \mathbb{C} \setminus \{0\}$ except for finitely many $s \in (0, 1)$ and for such $s \in (0, 1)$ the following events happen:

- (I_0) birth or death of loops around the origin through cusps at the origin;
- (I_∞) birth or death of exterior loops through cusps at the boundary of the Hill's region;
- (II^+) crossings through inverse self-tangencies;
- (III) crossings through triple points, see Figure 5.

Remark 2.5. By [7, Lemma 1], along a family of periodic orbits above \mathcal{K}_c^u , birth or death of interior loops which do not wind the origin can happen. We denote by $(I_{-\infty})$ this event. Note that the event $(I_{-\infty})$ does not happen during a Stark-Zeeman homotopy and the invariants \mathcal{J}_1 and \mathcal{J}_2 might change under this event, see Sections 4 and 5.

For a generic immersion $K \subset \mathbb{C}^*$, we write $w_0(K) \in \mathbb{Z}$ for the *winding number around the origin*. The **\mathcal{J}_1 invariant** is defined by

$$\mathcal{J}_1(K) := J^+(K) + \frac{(w_0(K))^2}{2}.$$

Recall that the *Levi-Civita regularization map* is given by the complex squaring map

$$L : \mathbb{C}^* \rightarrow \mathbb{C}^*, \quad v \mapsto v^2.$$

Note that for a generic immersion $K \subset \mathbb{C}^*$ the preimage $L^{-1}(K) \subset \mathbb{C}^*$ is also a generic immersion. Since the restriction $L|_{L^{-1}(K)} : L^{-1}(K) \rightarrow K$ is a 2-fold covering, the preimage $L^{-1}(K)$ has at most two components. The **\mathcal{J}_2 invariant** is then defined as follows.

If $w_0(K)$ is *odd*, then $L^{-1}(K)$ is connected and it is a single generic immersion. In this case we set

$$\mathcal{J}_2(K) := J^+(L^{-1}(K)).$$

If $w_0(K)$ is *even*, then $L^{-1}(K)$ consists of two components, i.e., two copies of a generic immersion. Choose one generic immersion \tilde{K} of $L^{-1}(K)$ and we set

$$\mathcal{J}_2(K) := J^+(\tilde{K}).$$

Since L is the complex squaring map, the two generic immersions of $L^{-1}(K)$ are related by a π -rotation in \mathbb{C}^* . This implies that $\mathcal{J}_2(K)$ does not depend on the choice of \tilde{K} .

Proposition 2.6. ([7, Propositions 4 and 5]) *The two invariants \mathcal{J}_1 and \mathcal{J}_2 do not change during Stark-Zeeman homotopies.*

The relation between the invariants \mathcal{J}_1 and \mathcal{J}_2 are partially given as follows.

Proposition 2.7. ([7, Proposition 4.6]) *If $w_0(K)$ is odd, then $\mathcal{J}_2(K) = 2\mathcal{J}_1(K) - 1$.*

It is known that if $w_0(K)$ is even, the invariants \mathcal{J}_1 and \mathcal{J}_2 are completely independent. See [7, Proposition 4.7].

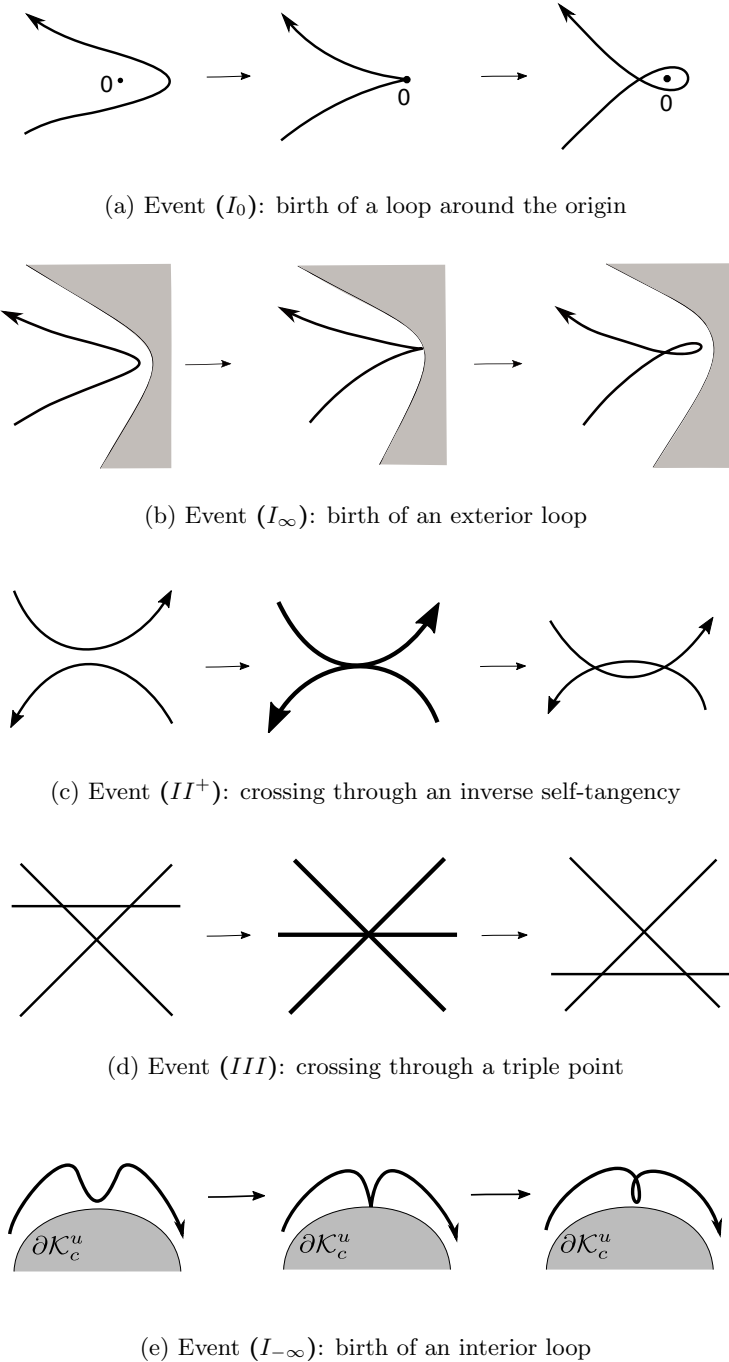


FIGURE 5. Possible events along a family of periodic orbits in a Stark-Zeeman system

3. THE ROTATING KEPLER PROBLEM

In this section, we study some properties of the rotating Kepler problem which we need to prove the main theorem. In particular, we see bifurcations of periodic orbits with negative Kepler energies.

In what follows, γ denotes a periodic orbit in the inertial Kepler problem and α a periodic orbit in the rotating Kepler problem.

We first fix some conventions. The symplectic form on $T^*\mathbb{R}^2$ with coordinates (q_1, q_2, p_1, p_2) is given by $\omega = dp_1 \wedge dq_1 + dp_2 \wedge dq_2$ and the Hamiltonian vector field X_H of a Hamiltonian H is defined by $\omega(X_H, \cdot) = -dH$. The Hamiltonian flow φ_H^t associated with the Hamiltonian H is defined to be a unique solution of the initial value problem: $(d/dt)\varphi_H^t(x) = X_H(\varphi_H^t(x))$ and $\varphi_H^0(x) = x$ for all x .

3.1. Hamiltonian and Integrals. Recall that the Hamiltonian of the restricted three body problem is given by

$$H_{3\text{BP}}(q, p) = \frac{1}{2}|p|^2 - \frac{1-\mu}{|q-E|} - \frac{\mu}{|q-M|} + q_1p_2 - q_2p_1,$$

where $E = (\mu, 0)$ is the Earth, $M = (-(1-\mu), 0)$ is the Moon and μ is the mass ratio of the two primaries. The rotating Kepler problem arises as the limit of this problem if we switch off the Moon, in other words, the mass ratio μ goes to zero. It follows that the Hamiltonian of the rotating Kepler problem is given by $H = E + L : T^*(\mathbb{R}^2 \setminus \{(0, 0)\}) \rightarrow \mathbb{R}$, where

$$E(q, p) = \frac{1}{2}|p|^2 - \frac{1}{|q|}$$

is the Hamiltonian of the inertial Kepler problem and

$$L(q, p) = q_1p_2 - q_2p_1$$

is the angular momentum. Note that the two quantities E and L are integrals of the system, namely $\{H, E\} = \{H, L\} = 0$, where $\{\cdot, \cdot\}$ means the Poisson bracket of two smooth functions. In particular, by the Noether theorem they are constant along orbits: $E(\varphi_H^t(x)) = E(x)$ and $L(\varphi_H^t(x)) = L(x)$ for any x and t .

By completing squares, we see that

$$H(q, p) = \frac{1}{2}((p_1 - q_2)^2 + (p_2 + q_1)^2) + U_{\text{eff}}(q),$$

where

$$U_{\text{eff}}(q) = -\frac{1}{|q|} - \frac{1}{2}|q|^2$$

is the effective potential. The twisted terms in the momenta are due to the Coriolis force and the term $-(1/2)|q|^2$ in the effective potential is due to the centrifugal force. The Hamiltonian H admits an S^1 -family of critical points of the form $(q_1, q_2, q_2, -q_1)$, where $|q| = 1$. The associated energy level $c_J = -3/2$ will be called the critical Jacobi energy.

3.2. Hill's regions. Given $c \in \mathbb{R}$, the Hill's region associated with the energy level c is given by

$$\mathcal{K}_c := \pi(H^{-1}(c)) = \{q = (q_1, q_2) \in \mathbb{R}^2 \setminus \{(0, 0)\} : U_{\text{eff}}(q) \leq c\},$$

where $\pi : T^*(\mathbb{R}^2 \setminus \{(0, 0)\}) \rightarrow \mathbb{R}^2 \setminus \{(0, 0)\}$ is the projection along the fiber. Consider the function

$$(1) \quad f(r) = -\frac{1}{r} - \frac{1}{2}r^2, \quad r > 0.$$

For $c < c_J$, the equation $f(r) = c$ admits two roots $r_1 < 1 < r_2$ having the property that

$$\mathcal{K}_c = (D_{r_1} \setminus \{(0, 0)\}) \cup (\mathbb{R}^2 \setminus \text{int}(D_{r_2})),$$

where D_r is the closed disk centered at the origin with radius r . Note that \mathcal{K}_c consists of two connected components: a bounded component $D_{r_1} \setminus \{(0, 0)\}$ and a unbounded component $\mathbb{R}^2 \setminus \text{int}(D_{r_2})$. As c goes to c_J , the two radii r_1 and r_2 tend to 1. At $c = c_J$, we have $r_1 = r_2 = 1$ and then the Hill's region equals $\mathcal{K}_{c_J} = \mathbb{R}^2 \setminus (\{(0, 0)\} \cup \partial D_1)$. Finally for $c > c_J$, the equation $f(r) = c$ has no solution and hence $\mathcal{K}_c = \mathbb{R}^2 \setminus \{(0, 0)\}$.

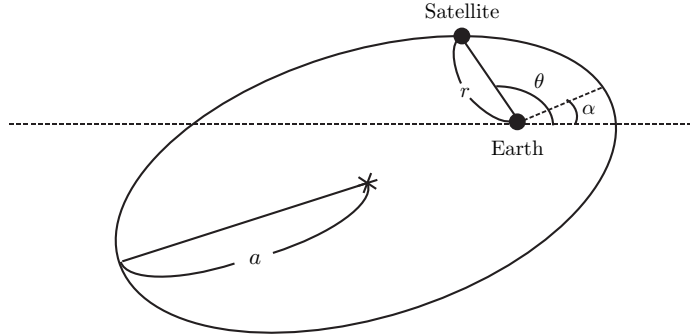


FIGURE 6. A Kepler ellipse

3.3. Periodic orbits. In the following we assume that the Kepler energy is negative, $E < 0$. Recall that if $E < 0$, then a periodic orbit in the inertial Kepler problem is either an elliptic orbit (including a collision orbit) or a circular orbit. Note that (noncollision) elliptic orbits are of the eccentricity $e \in (0, 1)$, collision orbits are of $e = 1$ and circular orbits are of $e = 0$.

Since $\{E, L\} = 0$, the two Hamiltonian flows X_E and X_L commute. It follows that the flow of their sums equals the composition of the flows of each vector field, namely

$$\varphi_H^t = \varphi_{E+L}^t = \varphi_E^t \circ \varphi_L^t = \varphi_L^t \circ \varphi_E^t.$$

It follows that an orbit α of the rotating Kepler problem is of the form $\alpha(t) = \exp(it)\gamma(t)$, where γ is an inertial Kepler orbit. Note that α is not necessarily periodic.

Suppose that γ is a Kepler ellipse of period $T > 0$. Then α is periodic if and only if there exist some relatively prime $k, l \in \mathbb{N}$ satisfying $kT = 2\pi l$. This implies that α is a k -fold covered Kepler ellipse in an l -fold covered coordinate system. In particular, it is $2\pi l$ -periodic. This observation gives rise to the following definition.

Definition 3.1. ([2, Section 4]) A τ -periodic orbit $\alpha(t) = \exp(it)\gamma(t)$ is called a $T_{k,l}$ -type orbit if $\tau = 2\pi l$ for some $l \in \mathbb{N}$ and $\gamma(t)$ is a Kepler ellipse of period T satisfying $kT = 2\pi l$. The family of all $T_{k,l}$ -type orbits is called the $T_{k,l}$ -torus family. Some examples of torus families are given in Figure 7.

Remark 3.2. Whenever $T_{k,l}$ -torus families are under consideration, we always assume that k and l are relatively prime. This implies that every $T_{k,l}$ -type orbit is simple covered.

Recall that a Kepler ellipse γ of energy E is described by the equation

$$(2) \quad r = \frac{a(1 - e^2)}{1 + e \cos(\theta - \alpha)},$$

where $r = |q|$, $a = -1/2E$ is the semi-major axis, θ is the angle between the major axis and the position vector and α is the argument of the perihelion, see Figure 6. It follows that the *perihelion* (the nearest point to the origin) of γ is of radius

$$r_{\min} = \frac{1 - e^2}{-2E(1 + e)} = \frac{1 - e}{-2E}$$

and the *aphelion* (the farthest point to the origin) is of radius

$$r_{\max} = \frac{1 - e^2}{-2E(1 - e)} = \frac{1 + e}{-2E}.$$

Since a $T_{k,l}$ -type orbit α is obtained from the k -fold covering of γ , there exist precisely k perihelions and k aphelions on α whose radii are given by

$$(3) \quad r_{\min} = \frac{1-e}{-2E_{k,l}} \quad \text{and} \quad r_{\max} = \frac{1+e}{-2E_{k,l}},$$

respectively.

Lemma 3.3. ([2, Section 6]) *The Kepler energy E is constant in each torus family.*

Proof. Let α and γ be as above. In view of the Kepler's third law $T^2 = (2\pi)^2/(-2E)^3$ and the fact that $kT = 2\pi l$, we obtain that $4\pi^2 l^2/k^2 = \pi^2/(-2E^3)$ which follows that $E = -(1/2)(k/l)^{2/3}$. This completes the proof of the lemma. \square

We denote by $E_{k,l}$ the Kepler energy of the $T_{k,l}$ -torus family, namely

$$(4) \quad E_{k,l} = -\frac{1}{2} \left(\frac{k}{l} \right)^{2/3}.$$

Observe that

$$(5) \quad \begin{cases} k > l & \text{if } E_{k,l} < -1/2 \\ k = l & \text{if } E_{k,l} = -1/2 \\ k < l & \text{if } -1/2 < E_{k,l} < 0. \end{cases}$$

Suppose that γ is a circular orbit. Since $\exp(it)$ takes circular orbits to circular orbits, $\alpha(t)$ is always a circular orbit. In particular, it is periodic. Recall that in the inertial Kepler problem, on each negative energy hypersurface there exist precisely two circular orbits, where one rotates counterclockwise and the other rotates clockwise. Note that in our convention the coordinate system rotates clockwise, see for example [1, Proposition 10.1.2]. A circular orbit in the rotating system is then called a *direct circular orbit* (or a *retrograde circular orbit*) if the associated circular orbit in the inertial system rotates clockwise (or counterclockwise). In other words, from the viewpoint of the inertial system, the direct circular orbit rotates in the same direction with the coordinate system and the retrograde circular orbit rotates in the opposite direction. This implies that a retrograde circular orbit has bigger angular momentum than a direct one.

Recall that the eccentricity e of a Kepler ellipse satisfies the relation

$$(6) \quad e^2 = 2EL^2 + 1 = 2E(H - E)^2 + 1.$$

Plugging $e = 0$ and $H = c$ into (6) gives rise to the equation

$$(7) \quad 2E(c - E)^2 + 1 = 0$$

whose graph consists of two connected components, see Figure 7. We abbreviate by Γ_l the left component and by Γ_r the right component in the figure. Each point on the graph represents a circular orbit in the rotating Kepler problem. Note that for every circular orbit the energy $H = c$ and the Kepler energy E cannot be equal. Indeed, if this is the case, then the left hand side of (6) becomes zero, while the right hand side is one. This implies that in view of the relation $c = E + L$, the circular orbits associated with a point on Γ_l (or Γ_r) is of negative angular momentum (or positive angular momentum). Consequently, Γ_l corresponds to direct circular orbits and Γ_r to retrograde circular orbits.

We now fix c . If $c < c_J$, then (7) has three solutions $E_1 < E_2 < -1/2 < E_3 < 0$. By the previous argument, we see that on the bounded connected component of the energy hypersurface $H^{-1}(c)$, there exist precisely one retrograde and one direct circular orbits, denote by C_{retro} and C_{direct} , whose Kepler energies are given by $E_{\text{retro}} := E_1$ and $E_{\text{direct}} := E_2$, respectively. On the unbounded component, there exists precisely one direct circular orbit of Kepler energy $E_{\text{direct}}^u := E_3$, which is denoted by C_{direct}^u . In view of the relation $0 = 2EL^2 + 1$, the angular momenta of C_{retro} , C_{direct} and C_{direct}^u are given by $L_{\text{retro}} = 1/\sqrt{-2E_{\text{retro}}}$, $L_{\text{direct}} = -1/\sqrt{-2E_{\text{direct}}}$ and $L_{\text{direct}}^u = -1/\sqrt{-2E_{\text{direct}}^u}$,

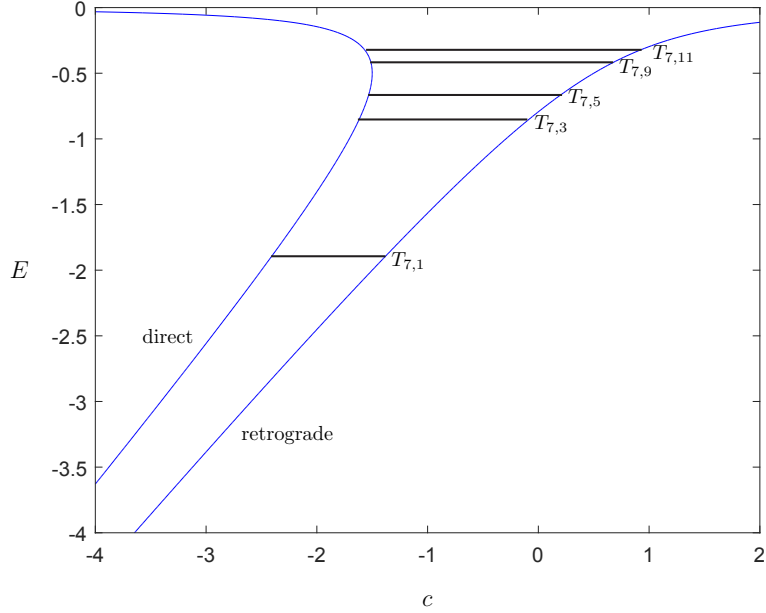


FIGURE 7. Some torus families for $k = 7$. The blue curves are the graph of the function $2E(c - E)^2 + 1 = 0$. The left curve is associated with direct circular orbits and the right one is associated with retrograde circular orbits. Observe that along each torus family, the energy level c is increasing.

respectively. On the other hand, since in the inertial system the semi-major axis of a Kepler ellipse equals $1/ - 2E$, on the bounded component of $H^{-1}(c)$, the radius of C_{direct} is bigger than that of C_{retro} .

3.4. Bifurcations of torus families. To see bifurcation of the torus families, we assume that $E = E_{k,l}$.

Proposition 3.4. ([2, Section 6 and Appendix B]) *The $T_{k,l}$ -torus family bifurcates from a $|k-l|$ -fold covered direct circular orbit and ends at a $(k+l)$ -fold covered retrograde circular orbit.*

Proof. We first claim that the period of a direct or retrograde circular orbit is given by

$$(8) \quad \tau_{\text{direct}} = \frac{2\pi l}{|k-l|} \quad \text{or} \quad \tau_{\text{retro}} = \frac{2\pi l}{k+l},$$

respectively. To see this, we introduce the polar coordinates (r, θ) so that $q_1 = r \cos \theta$ and $q_2 = r \sin \theta$. The momenta (p_r, p_θ) are defined by the canonical relation $p_1 dq_1 + p_2 dq_2 = p_r dr + p_\theta d\theta$. Note that the angular momentum is given by $L = p_\theta$. Under the coordinates change, the Hamiltonian becomes

$$(9) \quad H(r, \theta, p_r, p_\theta) = \frac{1}{2} \left(p_r^2 + \frac{p_\theta^2}{r^2} \right) - \frac{1}{r} + p_\theta$$

and the Hamiltonian vector field is given by

$$(10) \quad X_H = p_r \partial_r + \left(\frac{p_\theta}{r^2} + 1 \right) \partial_\theta + \frac{p_\theta^2 - r}{r^3} \partial_{p_r}.$$

Since the variable r is constant along circular orbits, we have $p_r = 0$ in (10). It then follows from the fact that p_r is constant that $p_\theta^2 = r$. Consequently, the Hamiltonian vector field along a circular

orbit is given by

$$X_H = \left(\frac{p_\theta}{r^2} + 1 \right) \partial_\theta.$$

In view of the initial conditions

$$r = \frac{1}{-2E} = \left(\frac{l}{k} \right)^{2/3}, \quad \theta = \theta_0, \quad p_r = 0, \quad p_\theta = \pm\sqrt{r},$$

we find the solutions

$$(11) \quad \begin{pmatrix} r \\ \theta \\ p_r \\ p_\theta \end{pmatrix} (t) = \begin{pmatrix} (l/k)^{2/3} \\ ((l \pm k)/l)t + \theta_0 \\ 0 \\ \pm(l/k)^{1/3} \end{pmatrix},$$

where the plus sign corresponds to retrograde circular orbits and the minus sign corresponds to direct circular orbits. The claim is now straightforward.

Recall that the angular momenta of the direct and retrograde circular orbits are given by $-1/\sqrt{-2E}$ and $1/\sqrt{-2E}$, respectively. This shows that the $T_{k,l}$ -torus family bifurcates from the (possibly multiple covered) direct circular orbit at

$$(12) \quad c = c_{k,l}^{\text{direct}} = E_{k,l} - 1/\sqrt{-2E_{k,l}}$$

and ends at the (possibly multiply covered) retrograde circular orbit at

$$c = c_{k,l}^{\text{retro}} = E_{k,l} + 1/\sqrt{-2E_{k,l}}.$$

Assume that the direct circular orbit is N -fold covered. Then we obtain the relation $N\tau_{\text{direct}} = 2\pi l$. By (8) we find

$$N = \frac{2\pi l}{\tau_{\text{direct}}} = |k - l|.$$

The assertion for the retrograde circular orbit can be proved in a similar way. This completes the proof of the proposition. \square

Remark 3.5. From (5) and (11) we see that direct circular orbits rotate clockwise for $E < -1/2$ (or equivalently $k > l$) and counterclockwise for $E > -1/2$ (or equivalently $k < l$). Retrograde circular orbits always rotate counterclockwise.

One can describe the bifurcation of the $T_{k,l}$ -torus family by varying the eccentricity as follows. At $e = 0$ which corresponds to the $|k - l|$ -fold covered direct circular orbit, $T_{k,l}$ -type orbits bifurcate. Such orbits will be referred to as *direct $T_{k,l}$ -type orbits*. Note that the winding number of direct $T_{k,l}$ -type orbits equals $l - k$. As e increases, they become more eccentric. The eccentricity increases until $e = 1$ at which collisions happen. After that event, the eccentricity decreases and we again obtain $T_{k,l}$ -type orbits, which will be referred to as *retrograde $T_{k,l}$ -type orbits*. Their winding number equals $k + l$. As e decreases, retrograde $T_{k,l}$ -type orbits become less eccentric and at $e = 0$ the $T_{k,l}$ -torus family ends at the $(k + l)$ -fold covered retrograde circular orbit. We call this e -parameter family the *e -homotopy*. We denote by I_{direct} the interval of increasing eccentricity for direct orbits and by I_{retro} the interval of decreasing eccentricity for retrograde orbits. In what follows, we think of those intervals as open, closed or half open intervals depending on situations. Note that this does not affect our argument.

3.5. Disasters. In this section, we examine which disasters happen during the e -homotopy.

3.5.1. Collisions. Fix any $T_{k,l}$ -torus family. It is obvious that collisions happen precisely at $e = 1$. Then by [7, Lemma 2] the event (I_0) happens only at $e = 1$.

3.5.2. *Hitting the boundary of the Hill's region.* In order to argue about the event (I_∞) , we first assume that $k > l$. We observe that in view of the equation (6) a direct $T_{k,l}$ -type orbit is of angular momentum $-\sqrt{1-e^2/-2E}$ and a retrograde $T_{k,l}$ -type orbit is of $\sqrt{1-e^2/-2E}$. Consequently, for $T_{k,l}$ -type orbits we have

$$(13) \quad c = E_{k,l} + L = \begin{cases} E_{k,l} - \sqrt{\frac{1-e^2}{-2E_{k,l}}} & \text{for } T_{k,l}\text{-type direct orbits} \\ E_{k,l} + \sqrt{\frac{1-e^2}{-2E_{k,l}}} & \text{for } T_{k,l}\text{-type retrograde orbits,} \end{cases}$$

where $E_{k,l}$ is given as in (4).

Since the eccentricity is decreasing on I_{retro} , the radius r_{\max} is decreasing for retrograde $T_{k,l}$ -type orbits. On the other hand, we abbreviate by R_c the radius of the boundary of the bounded component of the Hill's region associated with the energy level c . Since R_c is an increasing function on $c < c_J$, it is increasing on I_{retro} . For $e = 1$, we observe that

$$-\frac{1}{R_c} - \frac{1}{2}R_c^2 = E_{k,l}$$

and

$$r_{\max} = -\frac{1}{E_{k,l}}$$

from which we see that

$$\begin{aligned} -\frac{1}{R_c} - \frac{1}{2}R_c^2 = -\frac{1}{r_{\max}} &\Leftrightarrow \frac{1}{r_{\max}} - \frac{1}{R_c} = \frac{1}{2}R_c^2 \\ &\Rightarrow R_c - r_{\max} = \frac{1}{2}R_c^3 r_{\max} > 0. \end{aligned}$$

Therefore, retrograde $T_{k,l}$ -type orbits do not touch the boundary of the Hill's region.

For direct $T_{k,l}$ -type orbits, note that they touch the boundary of the bounded component of the Hill's region if and only if $r = r_{\max}$ solves the equation $f(r) = E_{k,l} - \sqrt{(1-e^2)/-2E_{k,l}}$, where the function f is defined as (1). We then compute that

$$\begin{aligned} -\frac{1}{r_{\max}} - \frac{1}{2}r_{\max}^2 = E_{k,l} - \sqrt{\frac{1-e^2}{-2E_{k,l}}} &\Leftrightarrow \frac{2E_{k,l}}{1+e} - \frac{(1+e)^2}{8E_{k,l}^2} - E_{k,l} = -\sqrt{\frac{1-e^2}{-2E_{k,l}}} \\ &\Leftrightarrow \frac{(1-e)E_{k,l}}{1+e} - \frac{(1+e)^2}{8E_{k,l}^2} = -\sqrt{\frac{1-e^2}{-2E_{k,l}}} \\ &\Leftrightarrow \frac{(1-e)^2 E_{k,l}^2}{(1+e)^2} + \frac{(1+e)^4}{64E_{k,l}^4} - \frac{1-e^2}{4E_{k,l}} = \frac{1-e^2}{-2E_{k,l}} \\ &\Leftrightarrow \frac{(1-e)^2 E_{k,l}^2}{(1+e)^2} + \frac{(1+e)^4}{64E_{k,l}^4} + \frac{1-e^2}{4E_{k,l}} = 0 \\ &\Leftrightarrow \left(\frac{(1-e)E_{k,l}}{(1+e)} + \frac{(1+e)^2}{8E_{k,l}^2} \right)^2 = 0 \\ &\Leftrightarrow 8(1-e)E_{k,l}^3 + (1+e)^3 = 0. \end{aligned}$$

The uniqueness of e solving this equation is obvious, which implies that during the e -homotopy for $k > l$, the event (I_∞) happens precisely once at $e = e_{k,l}^\infty \in I_{\text{direct}}$, see Figure 8.

We next assume that $k < l$. Observe that energies associated with retrograde $T_{k,l}$ -type orbits are bigger than the critical Jacobi energy. The Hill's regions are then given by $\mathcal{K}_c = \mathbb{R}^2 \setminus \{(0,0)\}$ and hence it has no boundary. Therefore, it suffices to consider direct $T_{k,l}$ -type orbits. Similar to the previous case, direct $T_{k,l}$ -type orbits touch the boundary of the unbounded component of the

Hill's region if and only if $r = r_{\min}$ solves the equation $f(r) = E_{k,l} - \sqrt{(1-e^2)/-2E_{k,l}}$. One can compute in a similar way that

$$-\frac{1}{r_{\min}} - \frac{1}{2}r_{\min}^2 = E_{k,l} - \sqrt{\frac{1-e^2}{-2E_{k,l}}} \Leftrightarrow 8(1+e)E_{k,l}^3 + (1-e)^3 = 0$$

which shows the same result as before, namely during the e -homotopy for $k < l$, the event $(I_{-\infty})$ happens precisely once at $e = e_{k,l}^{-\infty} \in I_{\text{direct}}$, see Figure 9.

3.5.3. Triple points. Suppose that q is an intersection point on a $T_{k,l}$ -type orbit of energy c . Then by (9) we have

$$p_r = \pm \sqrt{2\left(c + \frac{1}{|q|} - L\right) - \frac{L^2}{|q|^2}}.$$

The equation (10) then gives rise to

$$(14) \quad X_H(z) = \pm \sqrt{2\left(c + \frac{1}{|q|} - L\right) - \frac{L^2}{|q|^2}} \partial_r + \left(\frac{L}{|q|^2} + 1\right) \partial_\theta + \frac{L^2 - |q|}{|q|^3} \partial_{p_r}.$$

Since the angular momentum L is constant along the orbit, this shows that the intersection point q is double. We conclude that the event (III) does not happen in the rotating Kepler problem.

3.5.4. Self-tangencies. Suppose that a self-tangency happens at $q(t_0) = q(t_1)$ for $t_0 \neq t_1$. Since the tangent vectors are parallel at the self-tangency, in view of (14) we need to impose

$$(15) \quad L = -|q|^2.$$

From this we obtain the following two necessary conditions for the existence of self-tangencies:

- (i) the angular momentum is negative and hence the orbit is direct;
- (ii) $\sqrt{-L} \leq r_{\max}$ for the case $k > l$ and $\sqrt{-L} \geq r_{\min}$ for the case $k < l$, where r_{\max} and r_{\min} are defined as in (3).

It follows from (i) that the event (II^+) does not happen on I_{retro} .

Assume that the self-tangency at $q(t_0) = q(t_1)$ is direct. Since this point is also an intersection point, we have $r(t_0) = r(t_1)$ and $\theta(t_0) = \theta(t_1)$. Moreover, since $r(t_0) = r(t_1)$, it follows from (14) that $\dot{r}(t_0) = \dot{r}(t_1)$ and $\dot{\theta}(t_0) = \dot{\theta}(t_1) = 0$. Therefore, in view of the uniqueness theorem for second order ordinary differential equations, it follows that $t_0 = t_1$ which contradicts $t_0 \neq t_1$. Consequently, direct self-tangencies do not happen in the rotating Kepler problem.

Finally, we now consider an inverse self-tangency on I_{direct} . We assume that at $q(t_0) = q(t_1)$ an inverse self-tangency happens. Abbreviate $r_{\text{inv}} = |q(t_0)|$. Since the orbit is direct, we have $L = -\sqrt{(1-e^2)/-2E_{k,l}}$. By (15) we then obtain $r_{\text{inv}} = \sqrt[4]{(1-e^2)/-2E_{k,l}}$.

We first assume that $k > l$ and compute that

$$\begin{aligned} \sqrt[4]{\frac{1-e^2}{-2E_{k,l}}} < r_{\max} &\Leftrightarrow \sqrt[4]{1-e} < \sqrt[4]{\frac{1+e}{-2E_{k,l}}}^3 \\ &\Leftrightarrow 1-e < \left(\frac{1+e}{-2E_{k,l}}\right)^3 \\ &\Leftrightarrow 8(1-e)E_{k,l}^3 + (1+e)^3 > 0. \end{aligned}$$

Recall from Section 3.5.2 that $e = e_{k,l}^\infty$ is a unique solution of $8(1-e)E_{k,l}^3 + (1+e)^3 = 0$. Since $8(1-e)E_{k,l}^3 + (1+e)^3 > 0$ for $e > e_{k,l}^\infty$, this implies that if the event (II^+) is achieved at $e = e_0$, then we have $e_{k,l}^\infty < e_0$. One can easily obtain the same result with the event $(I_{-\infty})$ the case $k < l$.

We now claim that the event (II^+) must happen for $l \geq 2$. We first observe that if inverse self-tangencies occur along a direct $T_{k,l}$ -type orbit α , then they must lie on attached loops which are

born through cusps at the boundary of the Hill's region. To this end, we divide the trajectory of α into two parts: the first part α_{ext} is the union of k attached loops and the second part α_{int} is the remaining part. Note that along the part α_{int} the angular velocity $\dot{\theta}$ does not vanish. Since inverse self-tangencies happen precisely at points with $\dot{\theta} = 0$, this proves the observation.

Let γ be the Kepler ellipse of period T from which α is obtained. In view of $kT = 2\pi l$ we compute that

$$(16) \quad \alpha(t+T) = \exp(it+iT)\gamma(t+T) = \exp(2\pi il/k)\exp(it)\gamma(t) = \exp(2\pi il/k)\alpha(t).$$

In particular, the angle $|\arg(\alpha(0)) - \arg(\alpha(T))| = 2\pi l/k = T$, where $\arg(z)$ denotes the argument of $z \in \mathbb{C}$. By means of (16) it suffices to consider $t \in [0, T]$. Note that the two points $\alpha(0)$ and $\alpha(T)$ correspond to the perihelion of γ . Along γ , there exist precisely two points $\gamma(t_{\text{inv}})$ and $\gamma(T - t_{\text{inv}})$ such that $|\gamma(t_{\text{inv}})| = |\gamma(T - t_{\text{inv}})| = r_{\text{inv}}$. Since $r_{\text{inv}} = \sqrt[4]{(1-e^2)/-2E_{k,l}}$, for e sufficiently close to one, the time t_{inv} is so small that in view of (16) we have

$$(17) \quad T - \epsilon < |\arg(\alpha(t_{\text{inv}})) - \arg(\alpha(T - t_{\text{inv}}))| < T$$

for some $\epsilon > 0$ small enough.

We now suppose that $l \geq 2$ so that $T = 2\pi l/k > 2\pi/k$ and assume that the event (II^+) does not happen. In particular, no intersection points exist between attached loops. Since the number of attached loops equals k , it should hold that

$$|\arg(\alpha(t_{\text{inv}})) - \arg(\alpha(T - t_{\text{inv}}))| < \frac{2\pi}{k}$$

which contradicts (17) if e is close enough to 1. This proves the claim.

Remark 3.6. Numerical experiments show that the event (II^+) does not happen for the case $l = 1$ and happens precisely once for the case $l \geq 2$.

Recall that the e -homotopy of a $T_{k,l}$ -torus family is defined on $I_{\text{direct}} \cup I_{\text{retro}}$. We divide the interval I_{direct} into two subintervals: I_{direct}^1 from 0 to $e_{k,l}^\infty$ (or $e_{k,l}^{-\infty}$) and I_{direct}^2 from $e_{k,l}^\infty$ (or $e_{k,l}^{-\infty}$) to 1. All the results obtained so far prove the following.

Proposition 3.7.

- (i) The e -homotopy of a $T_{k,l}$ -torus family is generic on each interval I_{direct}^1 , I_{direct}^2 and I_{retro} .
- (ii) If $k > l$, then the e -homotopy is of Stark-Zeeman type, see Figure 8.
- (iii) If $k < l$, then the e -homotopy is a Stark-Zeeman homotopy on each interval I_{direct}^1 and $I_{\text{direct}}^2 \cup I_{\text{retro}}$, see Figure 9.

3.6. Symmetries.

Lemma 3.8. ([10, Section 8.2.1]) The trajectory of each $T_{k,l}$ -type orbit is invariant under the rotation by the angle $2\pi jl/k$, $j = 1, 2, \dots, k-1$.

Proof. It follows immediately from the fact that $kT = 2\pi l$ and (16). \square

On top of the rotational symmetry, trajectories of torus type orbits admit another symmetry.

Lemma 3.9. Assume that the perihelion of γ is the starting point $\gamma(0)$ and is of argument $\theta = \theta_0$. Then the trajectory of a $T_{k,l}$ -type orbit is invariant under the reflection with respect to the line $y = \tan(j\pi/k + \theta_0)x$, $j = 1, 2, \dots, k-1$. By convention, we regard the line $y = \tan(\pi/2)x$ as the y -axis.

Proof. Without loss of generality, we may assume that $\theta_0 = 0$. We first claim that the trajectory is symmetric under the reflection with respect to the x -axis. Indeed, we observe that

$$\overline{\alpha(t)} = \overline{\exp(it)\gamma(t)} = \exp(-it)\overline{\gamma(t)} = \exp(-it)\gamma(-t) = \alpha(-t).$$

In other words, the reflected orbit $\bar{\alpha}$ is the inverse of the original orbit α . This proves the claim.

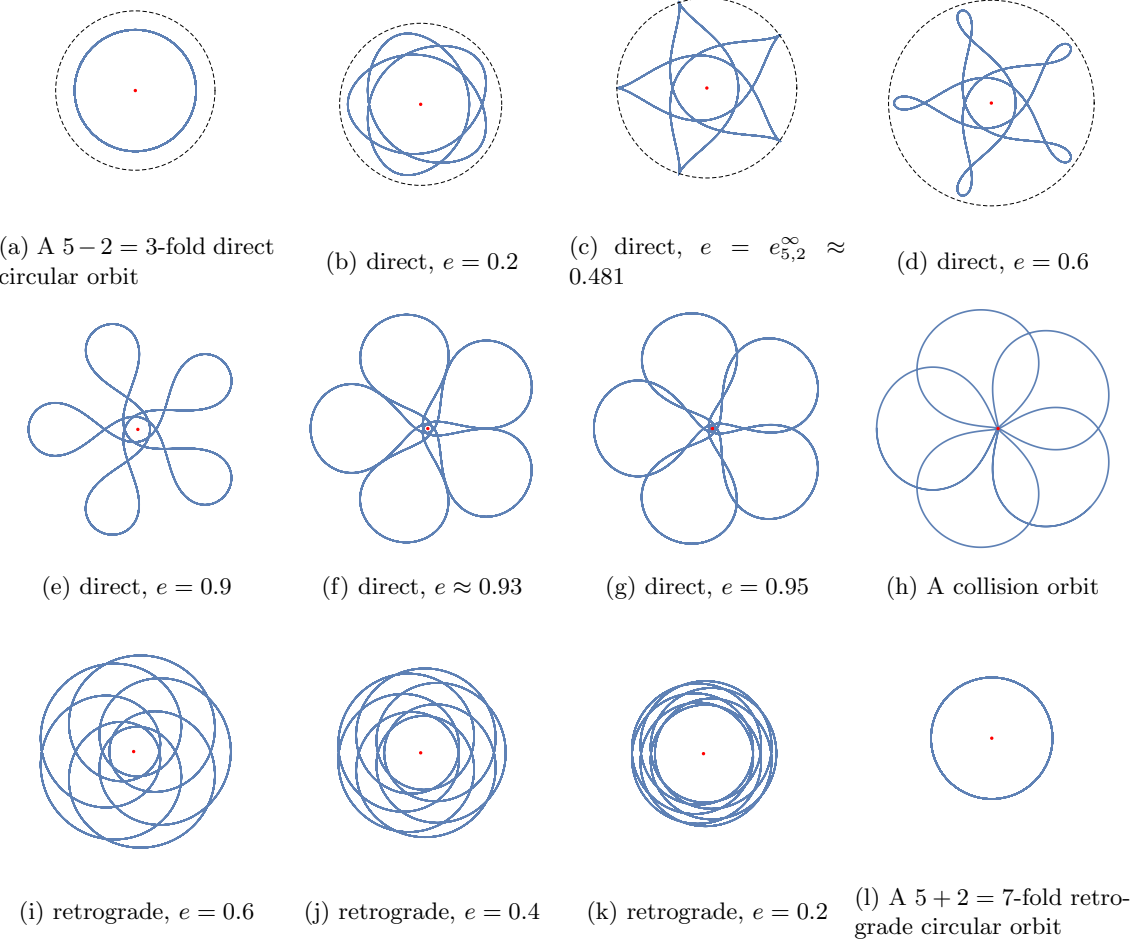


FIGURE 8. The e -homotopy of the $T_{5,2}$ -torus family. The dashed circles are the boundaries of the bounded components of the Hill's regions. In (e)-(l) no boundaries are indicated since the associated energies are bigger than the critical Jacobi energy $c_J = -3/2$. In (c) the direct $T_{5,2}$ -type orbit has cusps at the boundary of the Hill's region and then exterior loops appear in (d). Inverse self-tangencies are illustrated in (f). In (h) cusps at the origin happen and loops around the origin appear in (i).

Recall that the reflection matrix $\text{Ref}(\theta)$ with respect to the line $y = \tan(\theta)x$ is given by

$$\text{Ref}(\theta) = \begin{pmatrix} \cos 2\theta & \sin 2\theta \\ \sin 2\theta & -\cos 2\theta \end{pmatrix}.$$

One can easily check that the reflection and the rotation matrices satisfy the relation

$$\text{Rot}(\theta_1)\text{Ref}(\theta_2) = \text{Ref}\left(\frac{1}{2}\theta_1 + \theta_2\right).$$

Then the assertion follows from Lemma 3.8 and the claim by setting $\theta_1 = -2j\pi/k$ and $\theta_2 = j\pi/k$. This completes the proof of the lemma. \square

3.7. Trajectories of $T_{k,l}$ -type orbits. Without loss of generality we may assume that the perihelion of γ lies at the positive q_1 -axis. We parametrize it so that the perihelion is the starting point.

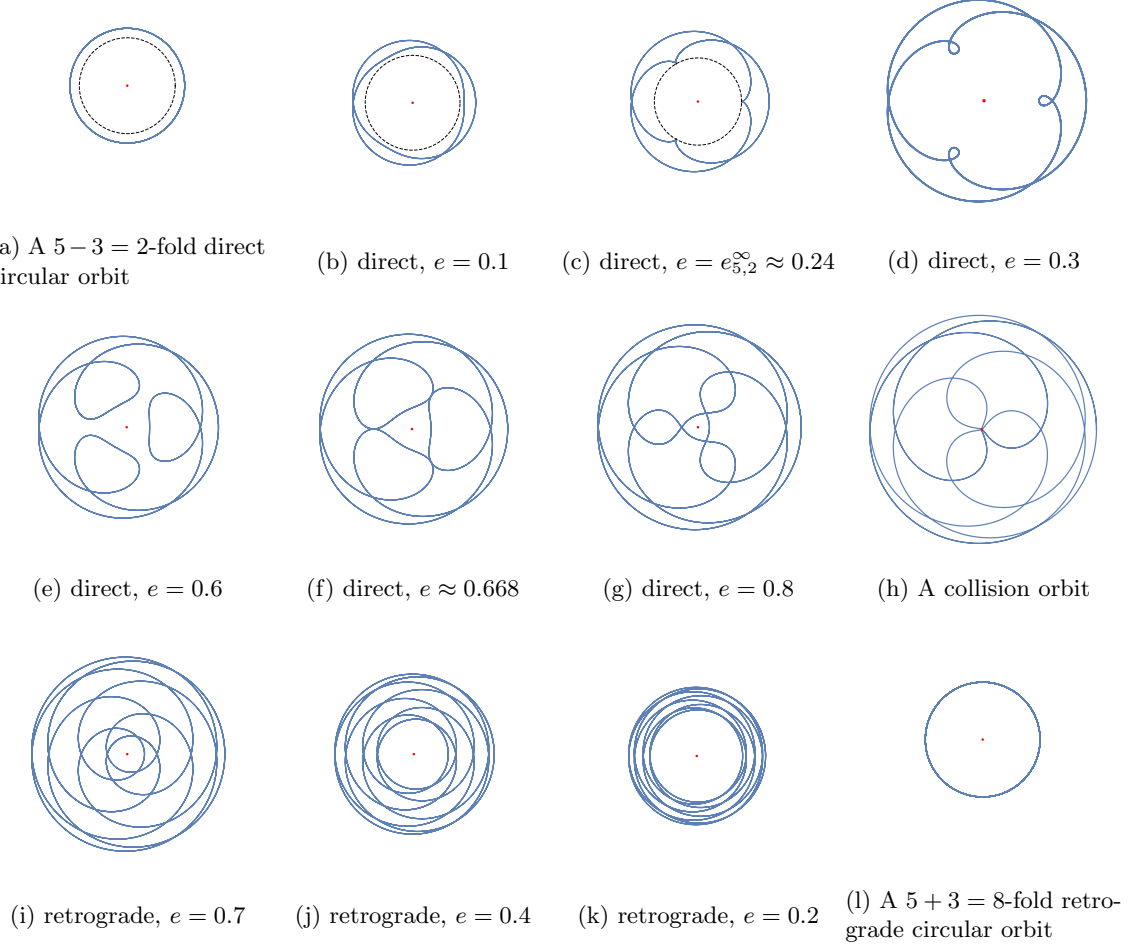


FIGURE 9. The e -homotopy of the $T_{3,5}$ -torus family. The dashed circles are the boundaries of the unbounded components of the Hill's regions. In (d)-(l) no boundaries are indicated since the associated energies are bigger than the critical Jacobi energy $c_J = -3/2$. In (c) the direct $T_{3,5}$ -type orbit has cusps at the boundary of the Hill's region and then interior loops appear in (d). Inverse self-tangencies are illustrated in (f). In (h) cusps at the origin happen and loops around the origin appear in (i).

Then by Lemma 3.8, since k and l are relatively prime, the set of arguments of the perihelions of α is given by

$$(18) \quad \left\{ 0, \frac{2\pi}{k}, \frac{4\pi}{k}, \dots, \frac{2(k-1)\pi}{k} \right\}.$$

Moreover, by (16) the set of times at which the massless body locates at the perihelions of α is given by

$$(19) \quad \left\{ 0, \frac{2\pi l}{k}, \frac{4\pi l}{k}, \dots, \frac{2(k-1)\pi l}{k} \right\}.$$

In order to argue with the aphelions, we observe that

$$\alpha(t + T/2) = \exp(it + iT/2)\gamma(t + T/2) = \exp(\pi il/k)\exp(it)\gamma(t + T/2).$$

Since $\arg(\gamma(t)) = \arg(\gamma(t + T/2)) + \pi$, we see that

$$\begin{aligned} \arg(\alpha(t + T/2)) &= \arg(\exp(\pi il/k)\exp(it)\gamma(t + T/2)) \\ &= \pi l/k + \arg(\alpha(t)) + \pi \\ &= \pi(k + l)/k + \arg(\alpha(t)). \end{aligned}$$

Therefore, the set of arguments of the aphelions equals the set (18) if $k + l$ is even and equals

$$(20) \quad \left\{ \frac{\pi}{k}, \frac{3\pi}{k}, \frac{5\pi}{k}, \dots, \frac{(2k-1)\pi}{k} \right\}$$

if $k + l$ is odd. Moreover, the set of times of the aphelions equals the set (19) if $k + l$ is even and equals

$$(21) \quad \left\{ \frac{\pi l}{k}, \frac{3\pi l}{k}, \frac{5\pi l}{k}, \dots, \frac{(2k-1)\pi l}{k} \right\}$$

if $k + l$ is odd. We summarize the results in the following.

Lemma 3.10. *Assume that the perihelion of γ is of argument $\theta = \theta_0$ and we parametrize γ so that the perihelion is achieved at $t = 0$. Then the following hold true:*

(i) *the sets of the perihelions and aphelions of α are given by*

$$\left\{ \alpha(t) : t = \frac{2j\pi l}{k}, j = 0, 1, 2, \dots, k-1 \right\}$$

and

$$\left\{ \alpha(t) : t = \frac{(2j+1)\pi l}{k}, j = 0, 1, 2, \dots, k-1 \right\},$$

respectively;

(ii) *assume that $k \pm l$ is even. Then the sets of arguments of the perihelions and aphelions of α are equal and given by*

$$(22) \quad \left\{ \theta : \theta = \theta_0 + \frac{2j\pi}{k}, j = 0, 1, 2, \dots, k-1 \right\}.$$

If $k \pm l$ is odd, then the set of arguments of the perihelions or the aphelions is given by (22) or by

$$(23) \quad \left\{ \theta : \theta = \theta_0 + \frac{(2j+1)\pi}{k}, j = 0, 1, 2, \dots, k-1 \right\},$$

respectively.

In what follows, we assume that the perihelion of γ lies on the positive q_1 -axis and is achieved at $t = 0$. In view of the rotational and reflection symmetries, to draw the trajectory of a $T_{k,l}$ -type orbit α it suffices to consider the part of the orbit which is contained in the sector

$$\{q \in \mathbb{C} : \arg(q) \in [0, \pi/k]\}.$$

Note that the radius of points on γ varies in $[r_{\min}, r_{\max}]$, where r_{\min} and r_{\max} are defined as in (3). Since we have assumed that the perihelion $\gamma(0)$ lies on the positive q_1 -axis, for each $r \neq r_{\min}, r_{\max}$, there exist precisely two points $\gamma(\pm t_r)$ such that $|\gamma(t_r)| = |\gamma(-t_r)| = r$. Therefore, since α is obtained from the k -fold covering of γ , for each $r \in (r_{\min}, r_{\max})$, there exist precisely $2k$ (possibly with intersections) points

$$(24) \quad \left\{ \alpha(t_r + \frac{2\pi jl}{k}) : j = 0, 1, 2, \dots, k-1 \right\} \cup \left\{ \alpha(-t_r + \frac{2\pi jl}{k}) : j = 0, 1, 2, \dots, k-1 \right\}$$

of radius r on α . If there exists an intersection between those points, i.e., $\alpha(t_r + 2\pi ml/k) = \alpha(-t_r + 2\pi nl/k)$ for some n, m , then by the rotational symmetry the two sets in (24) are identical, namely there exist k double points of radius r .

We have fixed the radius r and see how many points of α lies on the circle of radius r . In the following lemma we fix the angle θ_0 and see points of α which lies on the ray $\theta = \theta_0$.

Lemma 3.11. *Let α be a direct $T_{k,l}$ -type orbit of eccentricity $e < e_{k,l}^\infty$. For each $\theta_0 \in [0, 2\pi)$, there exist precisely $|k-l|$ points (possibly with multiple points) of α on the ray $\theta = \theta_0$. If α is retrograde, then there exist $(k+l)$ points (possibly with multiple points) having the same property.*

Proof. Since $e < e_{k,l}^\infty$, in view of the argument in Section 3.5, the angular velocity does not change the sign. Then the assertions follow from the fact that the winding number of direct or retrograde $T_{k,l}$ -type orbits equals $l-k$ and $k+l$, respectively. \square

We now determine on which rays double points lie.

Lemma 3.12. *Every double point of α is of argument $j\pi/k$ for some $j = 0, 1, 2, \dots, 2k-1$, provided that $e < e_{k,l}^\infty$ for direct $T_{k,l}$ -type orbits and that $e \in I_{\text{retro}}$ for retrograde $T_{k,l}$ -type orbits.*

Proof. Arguing indirectly we find a double point $\alpha(t_0) = \alpha(t_1)$ for some $t_0 \neq t_1$ which lies on the ray $\theta = \theta_0$ with $\theta_0 \neq j\pi/k$ for any j . Let j_0 be the angle such that

$$\frac{j_0\pi}{k} < \theta_0 < \frac{(j_0+1)\pi}{k}.$$

By means of the rotational symmetry, we may assume that $j_0 = 0$. Then the reflection symmetry shows that a double point also exists on the ray $\theta = -\theta_0$. By again the rotational symmetry we find $2k$ rays

$$\theta = \pm\theta_0, \pm\theta_0 + \frac{2\pi}{k}, \pm\theta_0 + \frac{4\pi}{k}, \dots, \pm\theta_0 + \frac{2(k-1)\pi}{k}$$

at which double points lie. By the argument before Lemma 3.11, the only possible case for θ_0 is

$$2\theta_0 = \theta_0 - (-\theta_0) = \frac{\pi}{k} \Rightarrow \theta_0 = \frac{\pi}{2k}.$$

Consider the part of the trajectory which lies in the region

$$(25) \quad \left\{ q \in \mathbb{R}^2 : \arg(q) \in \left[-\frac{\pi}{2k}, \frac{\pi}{2k} \right], r_{\min} \leq |q| \leq r_{\max} \right\}.$$

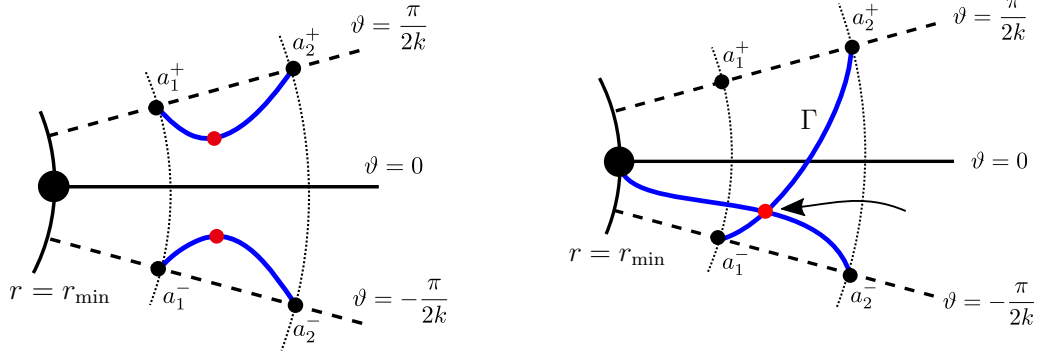
Suppose that we are considering a direct $T_{k,l}$ -type orbit. One can prove the same result for retrograde orbits. Recall that we have assumed that a perihelion is of argument $\theta = 0$. Points on the rays $\theta = -\pi/2k$ and $\theta = \pi/2k$ are of the form $a_j^- = r_j \exp(-i\pi/2k)$ and $a_j^+ = r_j \exp(i\pi/2k)$, respectively, for some $n < |k-l|$ and $r_1 < r_2 < \dots < r_n$. Since $e < e_{k,l}^\infty$, we see that $\dot{\theta}$ is never vanishing. Consequently, a_j^+ 's (or a_j^- 's) cannot be joined with each other by curves in the region (25), see Figure 10a.

Claim 1. a_1^\pm are connected with the perihelion.

Assume that there exists $j \geq 2$ such that a_j^- is connected with the perihelion. If a_1^- is joined with the perihelion, this makes the perihelion a double point, which is not the case. Suppose that a_1^- is joined with another point other than the perihelion by a curve Γ . Then the curve Γ should intersect the curve joining a_j^- and the perihelion. This gives rise to a new double point which does not lie on the ray of the form $\theta = j\pi/2k$, $j \in \mathbb{N}$, see Figure 10b. This contradiction impiles that such a $j \geq 2$ does not exist and hence a_1^- should be connected with the perihelion to obtain a closed trajectory. By the reflection symmetry, a_1^+ is also joined with the perihelion.

Claim 2. a_1^\pm are double points.

Assume by contradiction that they are single points. By the rotational symmetry, there exist n points b_j^- , $j = 1, 2, \dots, n$, such that $|b_j^-| = |a_j^-|$ on the ray $\theta = 3\pi/2k$. Note that b_1^- are connected



(a) The angular velocity $\dot{\theta}$ vanishes at the red points (b) The red point is a new double point which does not lie on the ray of the form $\theta = j\pi/2k$

FIGURE 10. Impossible cases

with a perihelion $r_{\min} \exp(2\pi/k)$. Consider the part of the orbit in $\pi/k \leq \theta \leq 3\pi/k$. Since at a_1^+ the radius is decreasing and $|a_1^+| = |b_1^-|$, the point a_1^+ should be joined with b_j^- for some $j \geq 2$. As before, if $j > 2$, then this gives rise to an additional double point which does not lie on the rays $\theta = j\pi/2k$, $j \in \mathbb{N}$. Therefore, a_1^+ is joined with b_2^- . By the reflection symmetry, b_1^- is joined with a_2^+ . We proceed similarly with a_2^+ and obtain that it is connected with a_3^- . By the reflection symmetry, a_2^- is joined with a_3^+ . Inductively, we join every point as in Figure 11. Regardless of the

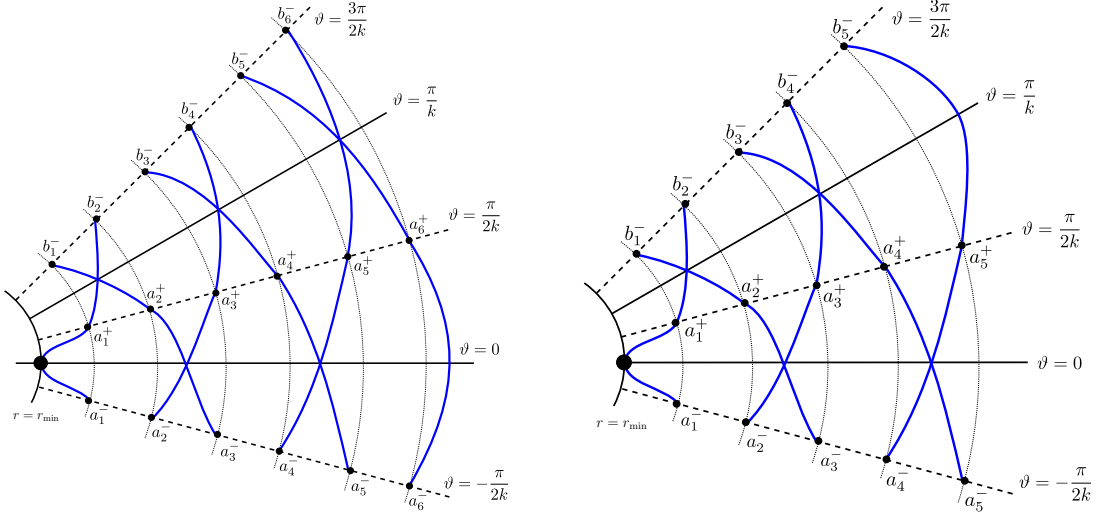


FIGURE 11. Every marked point is a single point

parity of $|k - l|$, we see that all points on the rays $\theta = \pm\pi/2k$ are single points. This contradiction proves the claim.

Since a_1^\pm are double points, they need to be connected with another points other than the perihelion. By the argument in the proof of the claim, we see that they are joined with a_2^\mp , respectively. As proceeding inductively, we join all the points as in Figure 12. Consider the curve joining a_1^+ and

a_2^- . Note that along this curve the radius is increasing. Following that curve in the inverse direction, we see that there must exist a point c with $|c| < |b_1^-| = |a_1^+|$ on the ray $\theta = 3\pi/2k$ such that a_1^+ is connected with c , see Figure 12. This contradicts to the fact that b_1^- is of the smallest radius among

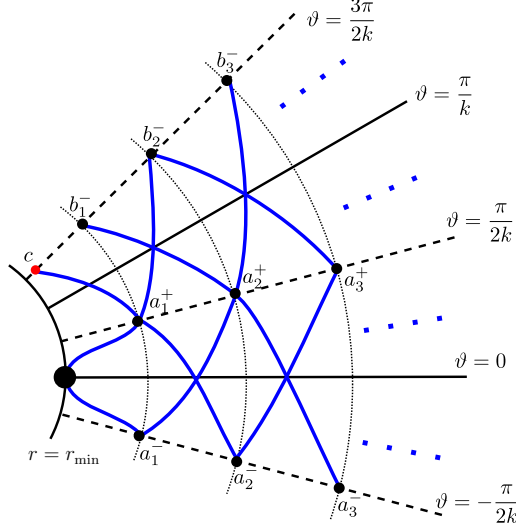


FIGURE 12. The red point c has the smallest radius among points on the ray $\theta = 3\pi/2k$

the points on $\theta = 3\pi/2k$. This completes the proof of the lemma. \square

Remark 3.13. The previous lemma also holds true for $e > e_{k,l}^\infty$ for direct $T_{k,l}$ -orbits. To see this, we first recall that the angular velocity vanishes only along attached loops. Then the proof of the previous lemma implies that every double point which does not lie on attached loops is of argument $j\pi/k$. If there exist no intersections between attached loops, then we have nothing to prove. Suppose that such intersections exist. Then the assertion follows from the fact that $|\arg(\alpha(jT + t_{\text{inv}})) - \arg(\alpha((j+1)T - t_{\text{inv}}))|$ is constant for all $j = 0, 1, 2, \dots, k-1$.

The next lemma can be easily proved by an argument similar as in the proof of the previous lemma.

Lemma 3.14. *Every point on each ray $\theta = j\pi/k$, $j = 0, 1, 2, \dots, 2k-1$, is either a perihelion, a aphelion or a double point.*

We now determine trajectories of torus type orbits. We only consider direct orbits. For retrograde orbits, one can show with $k+l$ instead of $|k-l|$ in a similar way. In view of the rotational and reflection symmetries, it suffices to consider the part of the curve in the region

$$\left\{ q \in \mathbb{R}^2 : \arg(q) \in [0, \frac{\pi}{k}], r_{\min} \leq |q| \leq r_{\max} \right\}.$$

Case 1. $|k-l|$ is odd.

Abbreviate $N = (|k-l|-1)/2$. By Lemma 3.10 on the ray $\theta = 0$ there exist the perihelion $a_0 = (r_{\min}, 0)$ and N double points a_1, a_2, \dots, a_N . On the other hand, on $\theta = \pi/k$, there exist another N points b_1, b_2, \dots, b_N and the aphelion $b_{N+1} = r_{\max} \exp(i\pi/k)$. Taking into account of the radial velocity \dot{r} , we obtain that

$$r_{\min} = |a_0| < |b_1| < |a_1| < |b_2| < |a_2| < \dots < |a_{N-1}| < |b_N| < |a_N| < |b_{N+1}| = r_{\max}.$$

Moreover, the point b_j is connected with a_{j-1} and a_j for $j = 1, 2, \dots, N$ and b_{N+1} is connected only with a_N . For convenience, we connected those points by straight lines, see Figure 13a.

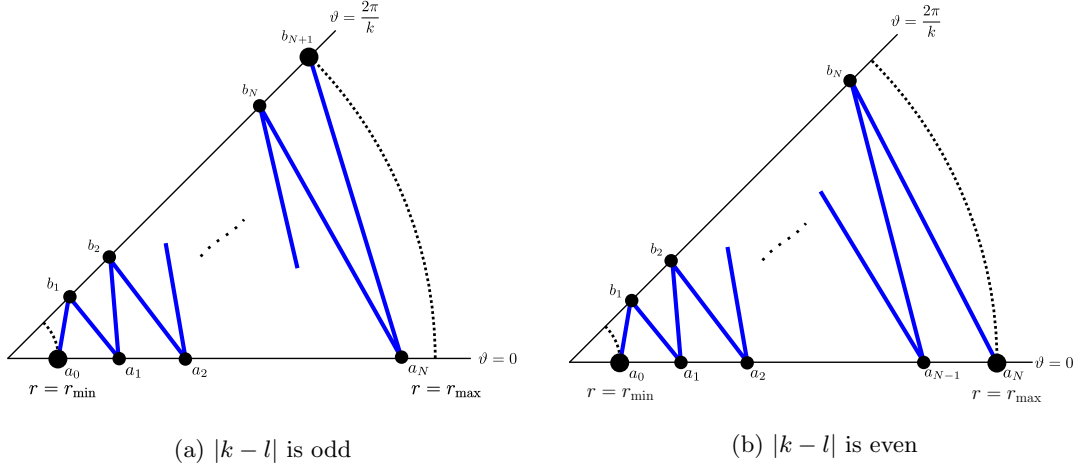


FIGURE 13. Connect the marked points

Case 2. $|k - l|$ is even.

Abbreviate $N = |k - l|/2$. Then on the ray $\theta = 0$ there exist the perihelion $a_0 = (r_{\min}, 0)$, the aphelion $a_N = (r_{\max}, 0)$ and $(N - 1)$ double points a_1, a_2, \dots, a_{N-1} . On the ray $\theta = \pi/k$, there exist N double points b_1, b_2, \dots, b_N . Those points satisfy

$$r_{\min} = |a_0| < |b_1| < |a_1| < |b_2| < |a_2| < \dots < |a_{N-1}| < |b_N| < |a_N| = r_{\max}.$$

In this case, b_j is connected with a_{j-1} and a_j for $j = 1, 2, \dots, N$. Also, we connect them by straight lines, see Figure 13b.

Using the rotational and reflection symmetries, we then obtain the trajectory of a direct $T_{k,l}$ -type orbit up to homotopy without any disaster. We denote the points on each ray $\theta = 2j\pi/k$ or $\theta = (2j + 1)\pi/k$ by the same letters a 's or b 's, respectively. Recall that we parametrize the orbit so that the perihelion $a_0 = (r_{\min}, 0)$ is the starting point. Then in view of the equation (16) we see that each time interval $[jT, (j+1)T]$ for $j = 0, 1, 2, \dots, l - 1$ is associated with a finite sequence of points

$$a_0, b_1, a_1, b_2, a_3, \dots, a_N, b_{N+1}, a_N, b_{N-1}, \dots, b_2, a_1, b_1, a_0$$

for the case $|k - l|$ is odd or

$$(26) \quad a_0, b_1, a_1, b_2, a_3, \dots, b_N, a_N, b_N, a_{N-1}, \dots, b_2, a_1, b_1, a_0$$

for the case $|k - l|$ is even, which corresponds to the eriod T of the underlying Kepler ellipse γ , see Figure 14.

Since we connect the marked points a 's and b 's on each ray $\theta = j\pi/k$ by straight lines, the obtained trajectory is not smooth. More precisely, the trajectory has a corner at each marked point. However, following the sequence (26) one can smoothen (with a small perturbation) the corners and then obtain a unique smooth trajectory which is a generic immersion up to homotopy without any disaster.

In Figure 15 we compare an original orbit in the rotating Kepler problem and an orbit obtained by the algorithms (before smoothing).

4. COMPUTATION OF THE J^+ -INVARIANT

Fix k and l which are relatively prime and consider the e -homotopy of the $T_{k,l}$ -torus family. By means of Proposition 3.7 and the fact that the J^+ -invariant is additive under connected sums, we

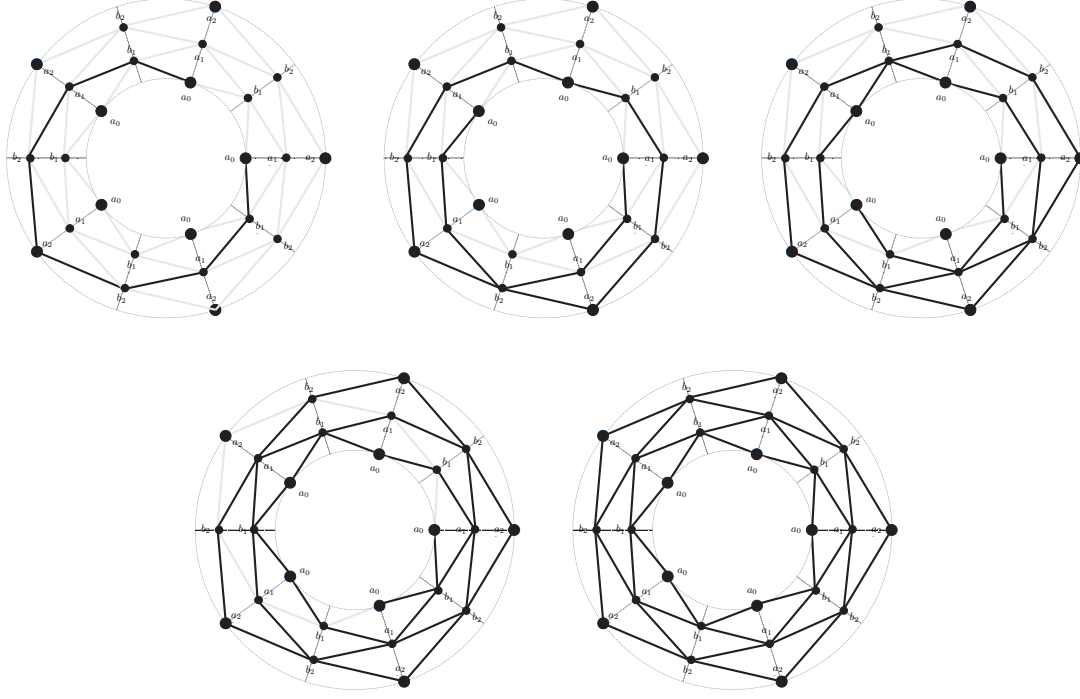


FIGURE 14. A direct $T_{5,1}$ -type orbit (before smoothing). The j th step corresponds to a j -fold coverd Kepler ellipse, $j = 1, 2, 3, 4, 5$.

just need to choose suitable representatives associated with I_{direct} and I_{retro} for the case $k > l$ and $I_{\text{direct}}^1, I_{\text{direct}}^2$ and I_{retro} for the case $k < l$.

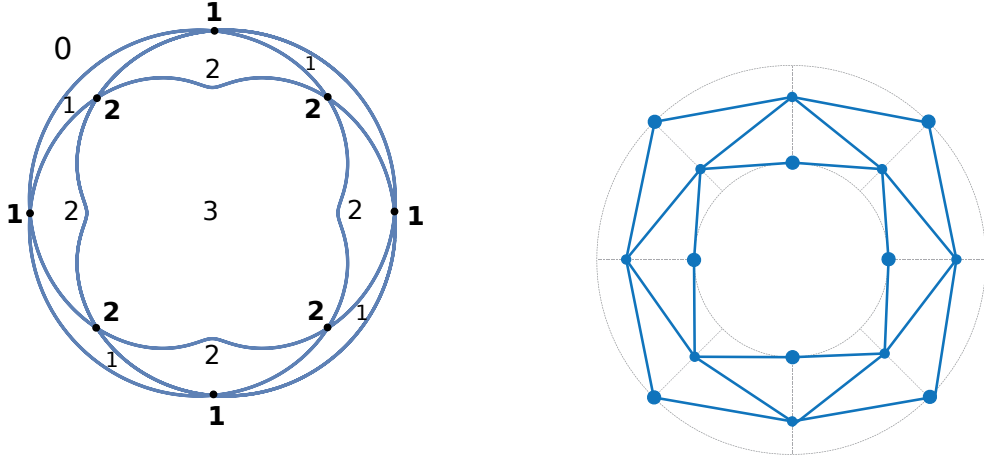
Case 1. On I_{direct} for $k > l$ or on I_{direct}^1 for $k < l$
 We choose $e \in I_{\text{direct}}^1$ for both cases $k > l$ and $k < l$. After obtaining the trajectory by the arguments in Section 3.7, we compute the J^+ -invariant using the Viro's formula which is given in Theorem 2.1. We first observe that the complement of the trajectory in \mathbb{R}^2 consists of $k(|k-l|-1) + 2$ connected components. The center component contains the origin and the most outside one is the unbounded component. The remaining $k(|k-l|-1)$ components form $(|k-l|-1)$ *layers* of bounded components, where each layer consists of k bounded components.

Choose $\theta_0 \neq j\pi/k$ for some j and rotate the curve by the angle $-j\pi/k$ so that the ray $\theta = \theta_0$ becomes the ray $\theta = 0$. Then the ray $\theta = 0$ can be written as the union

$$(0, d_0] \cup [d_0, d_1] \cup [d_1, d_2] \cup \cdots \cup [d_{|k-l|-2}, d_{|k-l|-1}] \cup [d_{|k-l|-1}, \infty)$$

according to intersections with the layers. We label each layer in such a way that *ith-layer* is the one which corresponds to the interval $[d_{i-1}, d_i]$ for $i = 1, 2, \dots, |k-l|-1$. The center and unbounded components are referred to as the *zeroth* and $|k-l|$ *th-layers*, respectively.

The winding number of each component is given as follows. Recall that the winding number of a component of the complement is defined to be the winding number of the curve around any interior point in the component. We first note that all components in the same layer are of the same winding number. Choose some $\theta_0 \neq j\pi/k$ as in the above. Since direct $T_{k,l}$ -type orbits always rotate in the same direction: clockwise for the case $k > l$ and counterclockwise for the case $k < l$, we see that the winding number of a component C equals the number of intersections between the trajectory and the ray $\theta = \theta_0$ starting at any point on $C \cap \{\theta = \theta_0\}$. We then conclude that the zeroth component



(a) A direct $T_{4,7}$ -type orbit of $e = 0.2$. The numbers in the interiors of the components mean their winding numbers and the bold ones are indices of the double points

(b) The orbit obtained by the algorithm

FIGURE 15. A direct $T_{4,7}$ -type orbit. There exist $4 \times (7 - 4 - 1) = 8$ double points and $7 - 4 - 1 = 2$ layers. Each layer is of 4 connected components. The winding number equals $7 - 4 = 3$.

is of winding number $l - k$ and the components in the i th layer are of winding number $l - k - i$. The $|k - l|$ th-layer has the winding number zero. Note that as we traverse from the zeroth layer to the $|k - l|$ th-layer, the winding number decreases by one.

We also label double points as follows. Recall that the double points can be divided into $(|k - l| - 1)$ subsets according to the associated radii. We order such radii in increasing order: $r_1 < r_2 < \dots < r_{|k - l| - 1}$, and the double points on the circle $r = r_j$ are then called j th double points, $j = 1, 2, \dots, |k - l| - 1$. Recall that the index of a double point is defined by the arithmetic mean of the winding numbers of adjacent components. Note that each j th double point is surrounded by four components: one in the $(j - 1)$ th layer, two in the j th layer and one in the $(j + 1)$ th layer. Since every component in the i th layer is of winding number $l - k - i$, we conclude that all the j th double points are of index

$$\frac{1}{4} \left((l - k - i + 1) + (l - k - i) + (l - k - i) + (l - k - i - 1) \right) = l - k - i,$$

see Figure 15.

By the Viro's formula the J^+ -invariant of the direct $T_{k,l}$ -type orbits is given by

$$\begin{aligned} J^+ &= 1 + k(|k - l| - 1) - \left(1 \cdot |k - l|^2 + k \cdot (|k - l| - 1)^2 + k \cdot (|k - l| - 2)^2 + \dots + k \cdot 1^2 \right) \\ &\quad + \left(k \cdot (|k - l| - 1)^2 + k \cdot (|k - l| - 2)^2 + \dots + k \cdot 1^2 \right) \\ &= 1 + k(|k - l| - 1) - |k - l|^2 \\ &= \begin{cases} 1 - k + kl - l^2 & \text{for } k > l \text{ and } I_{\text{direct}} \\ 1 - k - 2k^2 + 3kl - l^2 & \text{for } k < l \text{ and } I_{\text{direct}}^1 \end{cases} \end{aligned}$$

Case 2. On I_{direct}^2 for $k < l$

Abbreviate by α_j orbits for $e \in I_{\text{direct}}^j$, for $j = 1, 2$. Then α_2 looks like α_1 with k interior loops, which do not wind the origin, attached at each aphelion. In particular, the aphelions of α_1 become double points. It does not affect any difference on the winding numbers and indices of other components and double points, respectively. Since the winding number of the components enclosed by attached interior loops equals $l - k + 1$, the index of the new double points is given by

$$\frac{1}{4} \left((l - k + 1) + (l - k) + (l - k) + (l - k - 1) \right) = l - k.$$

Then in view of the computation in the case 1 we compute that

$$\begin{aligned} J^+ &= 1 - k - 2k^2 + 3kl - l^2 + k - k(l - k + 1)^2 + k(l - k)^2 \\ &= 1 - k + kl - l^2. \end{aligned}$$

Remark 4.1. One can compute the J^+ -invariant for the case 2 by using [7, Lemma 4]. Indeed, since k new born loops lie in the center component, their winding number is given by $l - k$. [7, Lemma 4] says that the J^+ -invariant for the case 2 differs from that for the case 1 with $l > k$ by $-2k(l - k)$. We then compute that

$$\begin{aligned} J^+(\text{Case 2}) &= J^+(\text{Case 1}) - 2k(l - k) \\ &= 1 - k - 2k^2 + 3kl - l^2 - 2kl + 2k^2 \\ &= 1 - k + kl - l^2. \end{aligned}$$

Case 3. On I_{retro} for both $k > l$ and $k < l$

Recall that for retrograde orbits, no disaster happens. Therefore, one can choose any eccentricity in I_{retro} . A similar argument as in the case 1 we conclude that the complement consists of $k(k+l-1)+2$ components and they consist of $(k+l+1)$ -layers: the zeroth layer (the center component), the $(k+l)$ th layer (the unbounded component) and $(k+l-1)$ layers, where each layer consists of k bounded components. The components in the i th layer are of winding number $k+l-i$ and then j th double points are of index $k+l-i$. We then compute that

$$\begin{aligned} J^+ &= 1 + k(k+l-1) - \left(1 \cdot (k+l)^2 + k \cdot (k+l-1)^2 + k \cdot (k+l-2)^2 + \cdots + k \cdot 1^2 \right) \\ &\quad + \left(k \cdot (k+l-1)^2 + k \cdot (k+l-2)^2 + \cdots + k \cdot 1^2 \right) \\ &= 1 + k(k+l-1) - (k+l)^2 \\ &= 1 - k - kl - l^2. \end{aligned}$$

We have proven

Proposition 4.2. *Let α be a $T_{k,l}$ -type orbit. Its J^+ -invariant is given by*

$$J^+(\alpha) = \begin{cases} 1 - k + kl - l^2 & \text{if } k > l \text{ and } \alpha \text{ is direct} \\ 1 - k - 2k^2 + 3kl - l^2 & \text{if } k < l \text{ and } e \in I_{\text{direct}}^1 \\ 1 - k + kl - l^2 & \text{if } k < l \text{ and } e \in I_{\text{direct}}^2 \\ 1 - k - kl - l^2 & \text{if } \alpha \text{ is retrograde} \end{cases}$$

Recall that periodic orbits of second kind (near the heavier primary) in the PCR3BP are obtained from $T_{k,l}$ -type orbits under a small perturbation of the mass ratio μ . Note that if μ is sufficiently small, the μ -perturbation (or μ -homotopy) is a generic homotopy without any disaster. In particular, the J^+ -invariant does not change during the μ -perturbation. We then obtain the following

Corollary 4.3. *Let α be a $T_{k,l}$ -type orbit. There exists a small $\mu_{k,l} > 0$ such that for any $\mu < \mu_{k,l}$ all periodic orbits δ of the second kind which are obtained from α has the same J^+ -invariant with α .*

5. COMPUTATION OF \mathcal{J}_1 AND \mathcal{J}_2 INVARIANTS

Recall that the winding number of retrograde or direct $T_{k,l}$ -type orbits is given by $k+l$ or $l-k$, respectively and then the formulas for \mathcal{J}_1 invariant follow from Proposition 4.2 and its definition.

In order to obtain \mathcal{J}_2 invariant, by definition, one should consider the Levi-Civita mapping $L : \mathbb{C}^* \rightarrow \mathbb{C}^*$, $z \mapsto z^2$. Let K be the trajectory of a $T_{k,l}$ -type orbit α . We parametrize α so that the starting point is one of the perihelions and assume that it lies on the positive q_1 -axis. We then observe that since L is a squaring map, the results in Section 3 give rise to the following:

- (i) the curve $L^{-1}(K)$ is invariant under the rotation by the angle $j\pi/k$ and is symmetric with respect to the line $y = (j\pi/2k)x$, $j = 0, 1, 2, \dots, 2k-1$, see Lemmas 3.8 and 3.9 ;
- (ii) if $k \pm l$ is odd, then the sets of the arguments of the perihelions and aphelions of $L^{-1}(K)$ are given by

$$(27) \quad \left\{ 0, \frac{\pi}{k}, \frac{2\pi}{k}, \dots, \frac{(2k-1)\pi}{k} \right\}$$

and

$$\left\{ \frac{\pi}{2k}, \frac{3\pi}{2k}, \dots, \frac{(4k-1)\pi}{2k} \right\},$$

respectively. If $k \pm l$ is even, then the two sets are equal and given by (27), see Lemma 3.10;

- (iii) if K is direct, for each $\theta_0 \in [0, 2\pi)$, there exist precisely $2|k-l|$ points (possibly with multiple points) of $L^{-1}(K)$ on the ray $\theta = \theta_0$, provided that $e < e_{k,l}^\infty$. If α is retrograde, then the same property holds true with $2(k+l)$, see Lemma 3.11;
- (iv) every double point is of argument $j\pi/2k$ for some $j = 0, 1, 2, \dots, 4k-1$, see Lemma 3.12 ;
- (v) given $r \in (\sqrt{r_{\min}}, \sqrt{r_{\max}})$, the number of points on $L^{-1}(K)$ with the radius r equals either $4k$ if the points are non-double points or $2k$ if the points are double points, where r_{\min} and r_{\max} is the radius minimum and maximum of K , respectively.

Case 1. Either $k > l$ or $k < l$ and I_{direct}^1 ; the winding number of K is odd.

Recall that the pulled back trajectory $L^{-1}(K)$ consists of a single curve and its winding number equals the winding number of K , i.e., $l-k$. Bearing the facts (i)-(v) in mind, one can draw $L^{-1}(K)$ by an algorithm similar to the one given in Section 3.7 with $2k(|k-l|-1)$ double points and $(|k-l|-1)$ layers. see Figure 16. It then follows from the Viro's formula that

$$\begin{aligned} \mathcal{J}_2(K) &= J^+(L^{-1}(K)) \\ &= 1 + 2k(|k-l|-1) - \left(1 \cdot |k-l|^2 + k \cdot (|k-l|-1)^2 + k \cdot (|k-l|-2)^2 + \dots + k \cdot 1^2 \right) \\ &\quad + \left(k \cdot (|k-l|-1)^2 + k \cdot (|k-l|-2)^2 + \dots + k \cdot 1^2 \right) \\ &= 1 + 2k(|k-l|-1) - |k-l|^2 \\ &= \begin{cases} (k-1)^2 - l^2 & \text{if } k > l \\ 1 - 2k - 3k^2 + 4kl - l^2 & \text{if } k < l \text{ and } I_{\text{direct}}^1 \end{cases} \end{aligned}$$

Case 2. $k < l$ and $I_{\text{direct}}^2 \cup I_{\text{retro}}$; the winding number K is odd.

We choose a retrograde $T_{k,l}$ -type orbit. Similar to the case 1, the pulled back trajectory $L^{-1}(K)$

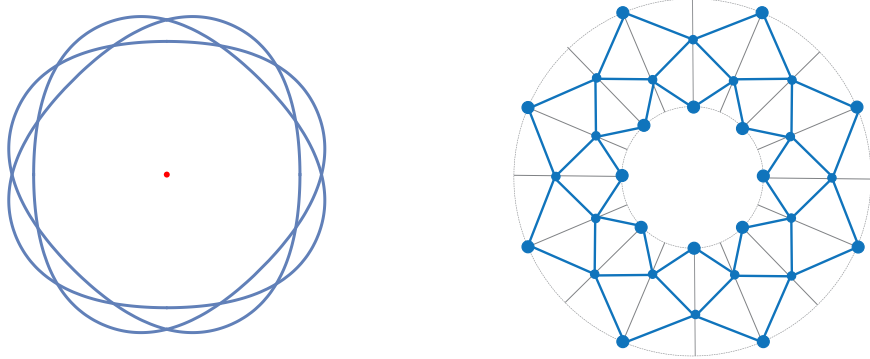
(a) A pulled back orbit of a direct $T_{4,1}$ -type orbit (b) An orbit obtained by the algorithm

FIGURE 16. A $L^{-1}(T_{4,1})$ -type orbit. There exist $(2 \times 4) \times (4 - 1 - 1) = 16$ double points and $4 - 1 - 1 = 2$ layers. Each layer is of $2 \times 4 = 8$ connected components. The winding number is $1 - 4 = -3$.

has $2k(k + l - 1)$ double points and $(k + l + 1)$ layers. Then we compute that

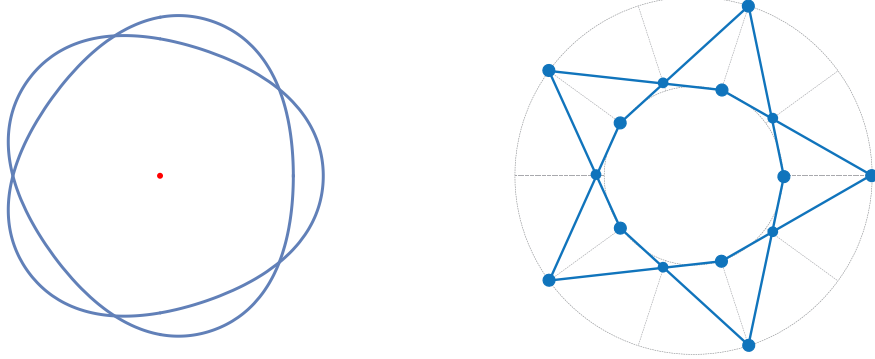
$$\begin{aligned}
 \mathcal{J}_2(K) &= 1 + 2k(k + l - 1) - \left(1 \cdot (k + l)^2 + k \cdot (k + l - 1)^2 + k \cdot (k + l - 2)^2 + \cdots + k \cdot 1^2 \right) \\
 &\quad + \left(k \cdot (k + l - 1)^2 + k \cdot (k + l - 2)^2 + \cdots + k \cdot 1^2 \right) \\
 &= 1 + 2k(k + l - 1) - (k + l)^2 \\
 &= (k - 1)^2 - l^2.
 \end{aligned}$$

Remark 5.1. Note that the formulas for the previous two cases equal the ones obtained by Proposition 2.7. For example, we compute that if $k > l$

$$\begin{aligned}
 \mathcal{J}_2(K) &= 2\mathcal{J}_1(K) - 1 \\
 &= 2 \left(1 - k + \frac{k^2}{2} - \frac{l^2}{2} \right) - 1 \\
 &= 1 - 2k + k^2 - l^2 \\
 &= (k - 1)^2 - l^2.
 \end{aligned}$$

Case 3. Either $k > l$ or $k < l$ and I_{direct}^1 ; the winding number K is even.

In this case $L : L^{-1}(K) \rightarrow K$ is also a 2–1 covering, but $L^{-1}(K)$ consists of two generic immersions. Fact (ii) shows that the two curves are related by π/k -rotation. Since the definition of \mathcal{J}_2 invariant is independent of the choice of a representative curve, we may choose a component $L_0^{-1}(K)$ whose one of the perihelions lies on the positive q_1 -axis. We then draw $L_0^{-1}(K)$ by following K from $\theta = 0$ to π with doubled angular velocity. Consequently, we have $w_0(L_0^{-1}(K)) = (l - k)/2$. Moreover, there exist $(|k - l|/2 - 1)$ layers and hence there exist $k(|k - l|/2 - 1)$ double points, see Figure 17. By the Viro's formula \mathcal{J}_2 invariant is given by


(a) A pulled back orbit of a direct $T_{5,1}$ -type orbit

(b) An orbit obtained by the algorithm

FIGURE 17. A $L^{-1}(T_{5,1})$ -type orbit. There exist $5 \times (\frac{5-1}{2} - 1) = 5$ double points and $\frac{5-1}{2} - 1 = 1$ layer. Each layer is of 5 connected components. The winding number is $\frac{1-5}{2} = -2$.

$$\begin{aligned}
\mathcal{J}_2(K) &= J^+(L_0^{-1}(K)) \\
&= 1 + k \left(\frac{|k-l|}{2} - 1 \right) - \left(1 \cdot \left(\frac{|k-l|}{2} \right)^2 + k \cdot \left(\frac{|k-l|}{2} - 1 \right)^2 + \dots + k \cdot 1^2 \right) \\
&\quad + \left(k \cdot \left(\frac{|k-l|}{2} - 1 \right)^2 + k \cdot \left(\frac{|k-l|}{2} - 2 \right)^2 + \dots + k \cdot 1^2 \right) \\
&= 1 + k \left(\frac{|k-l|}{2} - 1 \right) - \left(\frac{|k-l|}{2} \right)^2 \\
&= \begin{cases} 1 - k + \frac{1}{4}(k^2 - l^2) & \text{if } k > l \\ 1 - k - k^2 + \frac{3}{2}kl - \frac{1}{2}l^2 & \text{if } k < l \text{ and } I_{\text{direct}}^1 \end{cases}
\end{aligned}$$

Case 4. $k < l$ and $I_{\text{direct}}^2 \cup I_{\text{retro}}$; the winding number K is even.

Similarly, for a retrograde $T_{k,l}$ -type orbit K , we see that $w_0(L_0^{-1}(K)) = (l+k)/2$ and there exist $((k+l)/2 - 1)$ layers and $k((k+l)/2 - 1)$ double points. We then compute that

$$\begin{aligned}
\mathcal{J}_2(K) &= J^+(L^{-1}(K)) \\
&= 1 + k \left(\frac{k+l}{2} - 1 \right) - \left(1 \cdot \left(\frac{k+l}{2} \right)^2 + k \cdot \left(\frac{k+l}{2} - 1 \right)^2 + \dots + k \cdot 1^2 \right) \\
&\quad + \left(k \cdot \left(\frac{k+l}{2} - 1 \right)^2 + k \cdot \left(\frac{k+l}{2} - 2 \right)^2 + \dots + k \cdot 1^2 \right) \\
&= 1 + k \left(\frac{k+l}{2} - 1 \right) - \left(\frac{k+l}{2} \right)^2 \\
&= 1 - k - \frac{kl}{2} - \frac{l^2}{2}.
\end{aligned}$$

We have proven

Proposition 5.2. *Let α be a $T_{k,l}$ -type orbit. Its \mathcal{J}_1 and \mathcal{J}_2 invariants are given by*

$$\mathcal{J}_1(\alpha) = \begin{cases} 1 - k + \frac{k^2}{2} - \frac{l^2}{2} & \text{if } k > l \text{ or if } k < l \text{ and } \alpha \text{ is retrograde} \\ 1 - k - \frac{3}{2}k^2 + 2kl - \frac{1}{2}l^2 & \text{if } k < l \text{ and } e \in I_{\text{direct}}^1 \\ 1 - k + \frac{k^2}{2} - \frac{l^2}{2} & \text{if } k < l \text{ and } e \in I_{\text{direct}}^2 \end{cases}$$

$$\mathcal{J}_2(\alpha) = \begin{cases} (k-1)^2 - l^2 & \text{if } k > l \text{ and } w(\alpha) \text{ is odd} \\ 1 - k + \frac{k^2}{4} - \frac{l^2}{4} & \text{if } k > l \text{ and } w(\alpha) \text{ is even} \\ 1 - 2k - 3k^2 + 4kl - l^2 & \text{if } k < l, e \in I_{\text{direct}}^1 \text{ and } w(\alpha) \text{ is odd} \\ (k-1)^2 - l^2 & \text{if } k < l, e \in I_{\text{direct}}^2 \cup I_{\text{retro}} \text{ and } w(\alpha) \text{ is odd} \\ 1 - k - k^2 + \frac{3}{2}kl - \frac{1}{2}l^2 & \text{if } k < l, e \in I_{\text{direct}}^1 \text{ and } w(\alpha) \text{ is even} \\ 1 - k - \frac{1}{2}kl - \frac{1}{2}l^2 & \text{if } k < l, e \in I_{\text{direct}}^2 \cup I_{\text{retro}} \text{ and } w(\alpha) \text{ is even,} \end{cases}$$

where $w(\alpha)$ denotes the winding number of α .

By the argument before Corollary 4.3 we obtain the following

Corollary 5.3. *Let α be a $T_{k,l}$ -type orbit. There exists a small $\mu_{k,l} > 0$ such that for any $\mu < \mu_{k,l}$ all periodic orbits δ of the second kind which are obtained from α has the same invariants \mathcal{J}_1 and \mathcal{J}_2 with α .*

REFERENCES

- [1] R. Abraham and J. Marsden, *Foundations of Mechanics*, 2nd ed., Addison-Wesley, Reading (1978).
- [2] P. Albers, J. Fish, U. Frauenfelder and O. van Koert, *The Conley-Zehnder indices of the rotating Kepler problem*, Math. Proc. Cambridge Philos. Soc. (2013), 243–260.
- [3] R. F. Arenstorf, *Periodic solutions of the restricted three body problem representing analytic continuation of Keplerian elliptic motions*, Amer. J. Math., **85** (1963), 27–35.
- [4] V. I. Arnold, *Topological invariant of plane curves and caustics*, AMS Univ. Lecture Series Vol. 5 (1994).
- [5] R. Barrar, *Existence of periodic orbits of the second kind in the restricted problem of three bodies*, Astronom. J. **70** (1965), 3–4.
- [6] G. D. Birkhoff, *The restricted problem of three bodies*, Rend. Circ. Mat. Palermo, **39** (1915), 265–334.
- [7] K. Cieliebak, U. Frauenfelder and O. van Koert, *Periodic orbits in the restricted three-body problem and Arnold's J^+ -invariant*, Regul. Chaotic Dyn. **22** (2017), 408–434.
- [8] G. Darwin, *Periodic orbits*, Acta Math. **21** (1897), 99–242.
- [9] G. Darwin, *On certain families of periodic orbits*, Monthly Notices Roy. Astron. Soc. **70** (1909), 108–143.
- [10] U. Frauenfelder and O. van Koert, *The restricted three body problem and holomorphic curves*, book in preparation.
- [11] G. E. O. Giacaglia, *Periodic orbits of collision in the restricted problem of three bodies*, Astronomical J., **72** (1967), 386–391.
- [12] G. Hill, *Researches in the lunar theory*, Amer. J. Math. **1** (1878), 5–26, 129–147, 245–260.
- [13] A. Ljapunov, *Collected works*, Vol. I (Russian), Izdat. Akad. Nauk SSSR, Moscow (1954).
- [14] R. McGehee, *Some homoclinic orbits for the restricted three-body problem*, Thesis (Ph.D.)–The University of Wisconsin - Madison. 1969. 63 pp.
- [15] F. Moulton, *Periodic orbits*, Carnegie Inst. of Washington, Washington D.C. (1920).
- [16] H. Poincaré, *Les Méthodes Nouvelles de la Mécanique Céleste I-III*, Gauthiers-Villars, Paris (1899).
- [17] D. S. Schmidt, *Families of periodic orbits in the restricted problem of three bodies connecting families of direct and retrograde orbits*, SIAM J. Appl. Math., **22** no. 1 (1972), 27–37.
- [18] O. Viro, *Generic immersions of the circle to surfaces and the complex topology of real algebraic curves*, Amer. Math. Soc. Transl. Ser. 2 **173** (1996), 231–252.

DEPARTMENT OF MATHEMATICS AND RESEARCH INSTITUTE OF MATHEMATICS, SEOUL NATIONAL UNIVERSITY, BUILDING 27, ROOM 439, SAN 56-1, SILLIM-DONG, GWANAK-GU, SEOUL 151-747, SOUTH KOREA.

E-mail address: joontae@snu.ac.kr

UNIVERSITÄT AUGSBURG, UNIVERSITÄTSSTRASSE 14, D-86159 AUGSBURG, GERMANY

E-mail address: seongchan.kim@math.uni-augsburg.de